Journal of Computational Physics 385 (2019) 225–243

Contents lists available at ScienceDirect

Journal of Computational Physics

www.elsevier.com/locate/jcp

# A unified spectral method for FPDEs with two-sided derivatives; part I: A fast solver

Mehdi Samiee [a,b], Mohsen Zayernouri [a,b,*], Mark M. Meerschaert [c]

[a] Department of Computational Mathematics, Science, and Engineering, Michigan State University, 428 S.Shaw Lane, East Lansing, MI 48824, USA
[b] Department of Mechanical Engineering, Michigan State University, 428 S.Shaw Lane, East Lansing, MI 48824, USA
[c] Department of Statistics and Probability, Michigan State University, 619 Red Cedar Road Wells Hall, East Lansing, MI 48824, USA

ARTICLE INFO

*Article history:*
Received 24 October 2016
Received in revised form 24 January 2018
Accepted 2 February 2018
Available online 21 February 2018

*Keywords:*
Anomalous transport
High-dimensional FPDEs
Diffusion-to-wave dynamics
Jacobi poly-fractonomial
Unified fast solver
Spectral convergence

ABSTRACT

We develop a unified Petrov–Galerkin spectral method for a class of fractional partial differential equations with two-sided derivatives and constant coefficients of the form ${}_0\mathcal{D}_t^{2\tau}u + \sum_{i=1}^{d}[c_{l_i\,a_i}\mathcal{D}_{x_i}^{2\mu_i}u + c_{r_i\,x_i}\mathcal{D}_{b_i}^{2\mu_i}u] + \gamma\, u = \sum_{j=1}^{d}[\kappa_{l_j\,a_j}\mathcal{D}_{x_j}^{2\nu_j}u + \kappa_{r_j\,x_j}\mathcal{D}_{b_j}^{2\nu_j}u] + f$, where $2\tau \in (0,2)$, $2\tau \neq 1$, $2\mu_i \in (0,1)$ and $2\nu_j \in (1,2)$, in a $(1+d)$-dimensional *space–time* hypercube, $d = 1, 2, 3, \cdots$, subject to homogeneous Dirichlet initial/boundary conditions. We employ the eigenfunctions of the fractional Sturm–Liouville eigen-problems of the first kind in [1], called *Jacobi poly-fractonomials*, as temporal bases, and the eigen-functions of the boundary-value problem of the second kind as temporal test functions. Next, we construct our spatial basis/test functions using Legendre polynomials, yielding mass matrices being independent of the spatial fractional orders ($\mu_i$, $\nu_j$, $i$, $j = 1, 2, \cdots, d$). Furthermore, we formulate a novel unified fast linear solver for the resulting high-dimensional linear system based on the solution of generalized eigen-problem of spatial mass matrices with respect to the corresponding stiffness matrices, hence, making the complexity of the problem optimal, i.e., $\mathcal{O}(N^{d+2})$. We carry out several numerical test cases to examine the CPU time and convergence rate of the method. The corresponding stability and error analysis of the Petrov–Galerkin method are carried out in [2].

Published by Elsevier Inc.

## 1. Introduction

Fractional calculus seamlessly generalizes the notion of standard integer-order calculus to its fractional-order counterpart, leading to a broader class of mathematical models, namely fractional ordinary differential equations (FODEs) and fractional partial differential equations (FPDEs) [3–7]. Such non-local models appear as tractable mathematical tools to describe anomalous transport, which manifests in memory-effects, non-local interactions, power-law distributions, sharp peaks, and self-similar structures [8,4,9,10]. Although anomalous, such phenomena are observed in a range of applications e.g., bioengineering [11–15], turbulent flows [16–20], porous media [21–23], viscoelastic materials [24].

Due to their history dependence and non-local character, the discretization of such problems becomes computationally challenging. Numerical methods, developed to discretize FPDEs, can be categorized in two major classes: i) local methods,

* Corresponding author at: Department of Computational Mathematics, Science, and Engineering, Michigan State University, 428 S.Shaw Lane, East Lansing, MI 48824, USA.
*E-mail address:* zayern@msu.edu (M. Zayernouri).

https://doi.org/10.1016/j.jcp.2018.02.014
0021-9991/Published by Elsevier Inc.

e.g., finite difference method (FDM), finite volume method (FVM), and finite element method (FEM), and ii) global methods, e.g., single and multi-domain spectral methods (SM).

Local schemes have been studied extensively in the literature. Lubich introduced the discretized fractional calculus within the spirit of FDM [25]. Sugimoto employed a FDM scheme for approximating fractional Burger's equation [26,27]. Meerschaert and Tadjeran [28] developed finite difference approximations to solve one-dimensional advection–dispersion equations with variable coefficients on a finite domain. Tadjeran and Meerschaert [29] employed a practical alternating directions implicit (ADI) method to solve a class of fractional partial differential equations with variable coefficients in bounded domain. Hejazi et al., [30] developed a finite-volume method utilizing fractionally shifted Grunwald formula for the fractional derivatives for space-fractional advection–dispersion equation on a finite domain. To solve the two-dimensional two-sided space-fractional convection diffusion equation, Chen and Deng [31] proposed a practical alternating directions implicit method. Zeng et al., [32] constructed a finite element method and a multistep method for unconditionally stable time-integration of sub-diffusion problem. In addition, Zhao et al., developed second-order FDM for the variable-order FPDEs in [33]. Li et al., [34] proposed an implicit finite difference scheme for solving the generalized time-fractional Burger's equation. Recently, Feng et al., [35] proposed a second-order Crank–Nicolson scheme to approximate the Riesz space-fractional advection–dispersion equations (FADE). Moreover, two compact non-ADI FDMs have been proposed for the high-dimensional time-fractional sub-diffusion equation by Zeng et al., [36]. Recently, Zayernouri and Matzavinos [37] have developed an explicit fractional Adams/Bashforth/Moulton and implicit fractional Adams–Moulton finite difference methods, applicable to high-order time-integration of nonlinear FPDEs and amenable for formulating implicit/explicit (IMEX) splitting methods.

Regarding global methods, Sugimoto [26,27] used Fourier SM in a fractional Burger's equation. Shen and Wang [38] constructed a set of Fourier-like basis functions for Legendre–Galerkin method for non-periodic boundary value problems and proposed a new space–time spectral method. Sweilam et al., [39] considered Chebyshev Pseudo-spectral method for solving one-dimensional FADE, where the fractional derivative is described in Caputo sense. Chen et al., [40] developed an approach for high-order time integration within multi-domain setting for time-fractional diffusion equations. Mokhtary developed a fully discrete Galerkin method to numerically approximate initial value fractional integro-differential equations [41]. More recent works in this area can be found in [42–44].

Moreover, Zayernouri and Karniadakis [1,45] introduced a new family of basis/test functions, called *(tempered)Jacobi poly-fractonomials*, known as the explicit eigenfunctions of (tempered) fractional Strum-Liouville problems in bounded domains of the first and second kind. Following this new spectral theory, they have developed a number of single- and multi-domain spectral methods [46–50]. Recently, Dehghan et al. [51], employed a Galerkin finite element and interpolating element free Galerkin methods for full discretization of the fractional diffusion-wave equation and in [52] also introduced a full discretization of time-fractional diffusion and wave equations using meshless Galerkin method based on radial basis functions. Zaho et al., [53] developed a spectral method for the tempered fractional diffusion equations (TFDEs) using the generalized Jacobian function [54]. Mao and Shen [55] developed Galerkin spectral methods for solving multi-dimensional fractional elliptic equations with variable coefficients.

The main contribution of the present work is to construct a unified Petrov–Galerkin spectral method and a unified fast solver for the weak form of linear FPDEs with constant coefficients in (1+d) dimensional *space–time* hypercube of the form

$$ {}_0\mathcal{D}_t^{2\tau} u + \sum_{i=1}^{d} [c_{l_i\, a_i} \mathcal{D}_{x_i}^{2\mu_i} u + c_{r_i\, x_i} \mathcal{D}_{b_i}^{2\mu_i} u] = \sum_{j=1}^{d} [\kappa_{l_j\, a_j} \mathcal{D}_{x_j}^{2\nu_j} u + \kappa_{r_j\, x_j} \mathcal{D}_{b_j}^{2\nu_j} u] - \gamma\ u + f, \tag{1} $$

where $2\mu_i, \in (0,\ 1)$, $2\nu_i, \in (1,\ 2)$, and $2\tau, \in (0,\ 2)$, $2\tau \neq 1$, subject to Dirichlet initial and boundary conditions, where $i = 1,\ 2,\ \ldots,\ d$. Compared to the problem considered in [45], we extend the one-sided spatial derivatives to two-sided ones, also, we include an advection term in order to consider the drift effects. Employing different (Legendre polynomial) spatial basis/test functions and the additional advection term then would not allow employing the fast linear solver developed in [45]. Accordingly, we formulate a new fast linear solver for advection–dispersion problems. We additionally aim to perform the well-posedness and stability analysis in any (1+d) dimensions in [2], while in [45], only the stability of 1-D problem has been carried out. Furthermore, we briefly presented the stochastic interpretation of FADE on bounded domain which sheds light on the well-posedness of the problem from the perspective of the probability theory. In [2], we also carry out the corresponding error analyses of the PG method along with several verifying numerical tests.

The outline of this paper is as follows: in section 2, we introduce some preliminary results from fractional calculus. In section 3, we present the mathematical formulation of the spectral method in a (1+d) dimensional space, which leads to the generalized Lyapunov equations. In section 4, we develop a unified fast linear solver and obtain the closed-form solution in terms of the generalized eigenvalues and eigenvectors of the corresponding mass and stiffness matrices. In section 5, the performance of the PG method is examined via several numerical simulations for low-to-high dimensional problems with smooth and non-smooth solutions.

## 2. Preliminaries on fractional calculus

Here, we obtain some basic definitions from fractional calculus [4,49]. Denoted by ${}_a\mathcal{D}_x^{\sigma}\, g(x)$, the left-sided Reimann–Liouville fractional derivative of order $\nu$ in which $g(x) \in C^n[a,b]$ and $n = \lceil \sigma \rceil$, is defined as:

$$ {}^{RL}_{a}\mathcal{D}^{\sigma}_{x}\, g(x) = \frac{1}{\Gamma(n-\sigma)} \frac{d^n}{dx^n} \int_a^x \frac{g(s)}{(x-s)^{\sigma+1-n}}\, ds, \quad x \in [a,b], \tag{2} $$

where $\Gamma$ represents the Euler gamma function. The corresponding right-sided Reimann–Liouville fractional derivative of order $\nu$, ${}_{x}\mathcal{D}^{\sigma}_{b}\, g(x)$, is given by

$$ {}^{RL}_{x}\mathcal{D}^{\sigma}_{b}\, g(x) = \frac{1}{\Gamma(n-\sigma)} (-1)^n \frac{d^n}{dx^n} \int_x^b \frac{g(s)}{(s-x)^{\sigma+1-n}}\, ds, \quad x \in [a,b]. \tag{3} $$

In (2) and (3), as $\sigma \to n$, the fractional derivatives tend to the standard $n$-th order derivative with respect to $x$. We recall from [1,56] that the following link between the Reimann–Liouville and Caputo fractional derivatives, where

$$ {}^{Rl}_{a}\mathcal{D}^{\sigma}_{x}\, f(x) = \frac{f(a)}{\Gamma(1-\sigma)(x-a)^{\sigma}} + {}^{C}_{a}\mathcal{D}^{\sigma}_{x}\, f(x) \tag{4} $$

$$ {}^{Rl}_{x}\mathcal{D}^{\sigma}_{b}\, f(x) = \frac{f(b)}{\Gamma(1-\sigma)(b-x)^{\sigma}} + {}^{C}_{x}\mathcal{D}^{\sigma}_{b}\, f(x), \tag{5} $$

when $\lceil \sigma \rceil = 1$. Generally

$$ {}^{C}_{a}\mathcal{D}^{\sigma}_{x}\, f(x) = \frac{1}{\Gamma(n-\sigma)} \int_a^x \frac{g^{(n)}(s)}{(x-s)^{\sigma+1-n}}\, ds, \quad x \in [a,b], \tag{6} $$

$$ {}^{C}_{x}\mathcal{D}^{\sigma}_{b}\, f(x) = \frac{(-1)^n}{\Gamma(n-\sigma)} \int_x^b \frac{g^{(n)}(s)}{(s-x)^{\sigma+1-n}}\, ds, \quad x \in [a,b], \tag{7} $$

where $\lceil \sigma \rceil = n$. In (4) and (5), ${}^{RL}_{a}\mathcal{D}^{\sigma}_{x}\, g(x) = {}^{C}_{a}\mathcal{D}^{\sigma}_{x}\, g(x) = {}_{a}\mathcal{D}^{\sigma}_{x}\, g(x)$ when homogeneous Dirichlet initial and boundary conditions are enforced.

To analytically obtain the fractional differentiation of our basis function, we employ the following relations [1] as:

$$ {}^{RL}_{-1}\mathcal{I}^{\sigma}_{x} \{(1+x)^{\beta} P_n^{\alpha,\beta}(x)\} = \frac{\Gamma(n+\beta+1)}{\Gamma(n+\beta+\sigma+1)} (1+x)^{\beta+\sigma} P_n^{\alpha-\sigma,\beta+\sigma}(x), \tag{8} $$

and

$$ {}^{RL}_{x}\mathcal{I}^{\sigma}_{1} \{(1-x)^{\alpha} P_n^{\alpha,\beta}(x)\} = \frac{\Gamma(n+\alpha+1)}{\Gamma(n+\alpha+\sigma+1)} (1-x)^{\alpha+\sigma} P_n^{\alpha+\sigma,\beta-\sigma}(x), \tag{9} $$

where $0 < \sigma < 1$, $\alpha > -1$, $\beta > -1$ and $P_n^{\alpha,\beta}(x)$ denotes the standard Jacobi Polynomials of order n and parameters $\alpha$ and $\beta$. It is worth mentioning that

$$ {}^{RL}_{a}\mathcal{I}^{\sigma}_{x} \{f(x)\} = \frac{1}{\Gamma(\sigma)} \int_a^x \frac{f(s)}{(x-s)^{1-\sigma}}\, ds, \quad x \in [a,b], $$

and

$$ {}^{RL}_{x}\mathcal{I}^{\sigma}_{b} \{f(x)\} = \frac{1}{\Gamma(\sigma)} \int_x^b \frac{f(s)}{(s-x)^{1-\sigma}}\, ds, \quad x \in [a,b]. $$

By substituting $\alpha = \sigma$ and $\beta = -\sigma$, we can simplify equations (8) and (9), thereby we have:

$$ {}^{RL}_{-1}\mathcal{I}^{\sigma}_{x} \{(1+x)^{-\sigma} P_n^{\sigma,-\sigma}(x)\} = \frac{\Gamma(n-\sigma+1)}{\Gamma(n+1)} P_n(x), \quad x \in [-1,1] \tag{10} $$

and

$$ {}^{RL}_{x}\mathcal{I}^{\sigma}_{1} \{(1-x)^{-\sigma} P_n^{-\sigma,\sigma}(x)\} = \frac{\Gamma(n-\sigma+1)}{\Gamma(n+1)} P_n(x), \quad x \in [-1,1]. \tag{11} $$

Accordingly, we have the fractional derivative of Legendre polynomial by differentiating (10) and (11) as

$$ {}_{-1}\mathcal{D}^{\sigma}_{x}\, P_n(x) = \frac{\Gamma(n+1)}{\Gamma(n-\sigma+1)} P_n^{\sigma,-\sigma}(x)\, (1+x)^{-\sigma} \tag{12} $$

and

$$ {}_x\mathcal{D}_1^{\sigma} P_n(x) = \frac{\Gamma(n+1)}{\Gamma(n-\sigma+1)} P_n^{-\sigma,\sigma}(x)\,(1-x)^{-\sigma}, \tag{13} $$

where $P_n(x) = P_n^{0,0}(x)$ represents Legendre polynomial of degree n.

## 3. Mathematical framework

Let $u : \mathbb{R}^{d+1} \to \mathbb{R}$ for some positive integer $d$ and $\Omega = [0,T] \times [a_1,b_1] \times [a_2,b_2] \times \cdots \times [a_d,b_d]$, where

$$ {}_0\mathcal{D}_t^{2\tau} u + \sum_{i=1}^{d} \left[ c_{l_i\, a_i} \mathcal{D}_{x_i}^{2\mu_i} u + c_{r_i\, x_i} \mathcal{D}_{b_i}^{2\mu_i} u \right] - \sum_{j=1}^{d} \left[ \kappa_{l_j\, a_j} \mathcal{D}_{x_j}^{2\nu_j} u + \kappa_{r_j\, x_j} \mathcal{D}_{b_j}^{2\nu_j} u \right] + \gamma\, u = f, \tag{14} $$

and $\gamma, c_{l_i}, c_{r_i}, \kappa_{l_j}$, and $\kappa_{r_j}$ are all constant. Besides, $2\mu_i \in (0,1)$, $2\nu_j \in (1,2)$, and $2\tau \in (0,2)$, $2\tau \neq 1$, for $j = 1, 2, \cdots, d$. This equation is subject to the following Dirichlet initial and boundary conditions as:

$$ \begin{aligned} &u|_{t=0} = 0, \quad \tau \in (0, 1/2), \\ &u|_{t=0} = \frac{\partial u}{\partial t}|_{t=0} = 0, \quad \tau \in (1/2, 1), \\ &u|_{x_j=a_j} = u|_{x_j=b_j} = 0, \quad \nu_j \in (1/2, 1), \quad j = 1, 2, \cdots, d. \end{aligned} $$

### 3.1. Stochastic interpretation of the FPDEs

Following [57], we provide a brief stochastic interpretation of the FPDEs in (14) that further sheds light on the well-posedness of the problem from the perspective of probability theory. Let suppose that in (14), $f \equiv 0$ and $\gamma = 0$ and $0 < 2\tau < 1$ and that $a_i = -\infty$ and $b_i = +\infty$ for $i = 1, 2, \cdots$. Then (14) governs [57] a time-changed Lévy process $X(E_t)$ on $\mathbb{R}^d$ whose Fourier transform is $\mathbb{E}[e^{-ik\cdot X(t)}] = e^{t\psi(k)}$ with the Fourier symbol

$$ \psi(k) = -\sum_{n=1}^{d} [c_{l_n} (ik_n)^{2\mu_n} + c_{r_n} (-ik_n)^{2\mu_n}] + \sum_{m=1}^{d} [\kappa_{l_m} (-ik_m)^{2\nu_m} + \kappa_{r_m} (ik_m)^{2\nu_m}]. \tag{15} $$

Recalling that in one dimension the Lévy process $Y(t)$ with Fourier Transform $\mathbb{E}[e^{-ikY(t)}] = e^{t\psi_0(k)}$ where $\psi_0(k) = pD(ik)^{\alpha} + qD(-ik)^{\alpha}$ for $D > 0$ and $1 < \alpha \leq 2$, $p \geq 0$, $q \geq 0$, and $p + q = 1$ is a stable Lévy process with index $\alpha$ and skewness $p - q$ [4,57].

Then $X(t)$ has $d$ independent components, each of which is the sum of two independent stable Lévy processes with index $2\mu_m$ and $2\nu_m$, respectively. Furthermore, for a bounded domain $\Lambda_d$, letting $X'(t)$ denote the modification of the process $X(t)$ that vanishes the first time it leaves the domain, (14) governs the time-changed Markov process $X'(E_t)$. You can find complete details in [4].

### 3.2. Mathematical framework

In [58], the usual Sobolev space associated with the real index $\sigma \geq 0$ on bounded interval $\Lambda = (a,b)$, is denoted by $H^{\sigma}(\Lambda)$ and is defined as the completion of $C_0^{\infty}(\Lambda)$ with respect to the norm $\|\cdot\|_{H^{\sigma}(\Lambda)}$. As shown in Lemma 2.6 in [58], the equivalency between the following norms holds:

$$ \|\cdot\|_{H^{\sigma}(\Lambda)} \equiv \|\cdot\|_{{}^{l}H^{\sigma}(\Lambda)} \equiv \|\cdot\|_{{}^{r}H^{\sigma}(\Lambda)}, \tag{16} $$

where

$$ \|\cdot\|_{{}^{l}H^{\sigma}(\Lambda)} = \left( \|\, {}_a\mathcal{D}_x^{\sigma}(\cdot)\|_{L^2(\Lambda)}^2 + \|\cdot\|_{L^2(\Lambda)}^2 \right)^{\frac{1}{2}}, \tag{17} $$

and

$$ \|\cdot\|_{{}^{r}H^{\sigma}(\Lambda)} = \left( \|\, {}_x\mathcal{D}_b^{\sigma}(\cdot)\|_{L^2(\Lambda)}^2 + \|\cdot\|_{L^2(\Lambda)}^2 \right)^{\frac{1}{2}}. \tag{18} $$

Similarly, we can show that $\|\cdot\|_{H^{\sigma}(\Lambda)} \equiv \|\cdot\|_{{}^{c}H^{\sigma}(\Lambda)}$, defined as

$$ \|\cdot\|_{{}^{c}H^{\sigma}(\Lambda)} = \left( \|\, {}_x\mathcal{D}_b^{\sigma}(\cdot)\|_{L^2(\Lambda)}^2 + \|\, {}_a\mathcal{D}_x^{\sigma}(\cdot)\|_{L^2(\Lambda)}^2 + \|\cdot\|_{L^2(\Lambda)}^2 \right)^{\frac{1}{2}}. \tag{19} $$

Let $\Lambda_1 = (a_1, b_1)$, $\Lambda_i = (a_i, b_i) \times \Lambda_{i-1}$ for $i = 2, \cdots, d$, and $\mathcal{X}_1 = H_0^{\nu_1}(\Lambda_1)$, with the associated norm $\|\cdot\|_{H^{\nu_1}(\Lambda_1)} \equiv |\cdot|_{H^{\nu_1}(\Lambda_1)}$. Accordingly, we construct $\mathcal{X}_d$ such that

$$\begin{aligned}
&\mathcal{X}_2 = H_0^{\nu_2}\Big((a_2, b_2); L^2(\Lambda_1)\Big) \cap L^2((a_2, b_2); \mathcal{X}_1),\\
&\quad\vdots\\
&\mathcal{X}_d = H_0^{\nu_d}\Big((a_d, b_d); L^2(\Lambda_{d-1})\Big) \cap L^2((a_d, b_d); \mathcal{X}_{d-1}),
\end{aligned} \tag{20}$$

associated with the norm

$$\|\cdot\|_{\mathcal{X}_d} = \left\{\|\cdot\|^2_{L^2(\Lambda_d)} + \sum_{i=1}^{d}\Big(\|{}_{x_i}\mathcal{D}^{\nu_i}_{b_i}(\cdot)\|^2_{L^2(\Lambda_d)} + \|{}_{a_i}\mathcal{D}^{\nu_i}_{x_i}(\cdot)\|^2_{L^2(\Lambda_d)}\Big)\right\}^{\frac{1}{2}}. \tag{21}$$

Similarly, the Sobolev space with index $\tau > 0$ on the time interval $I = (0, T)$, denoted by $H^\tau(I)$, is endowed with norm $\|\cdot\|_{H^\tau(I)}$, where

$$\|\cdot\|_{H^\tau(I)} \equiv \|\cdot\|_{{}^lH^\tau(I)} \equiv \|\cdot\|_{{}^rH^\tau(I)}, \tag{22}$$

$$\|\cdot\|_{{}^lH^\tau(I)} = \Big(\|{}_0\mathcal{D}^\tau_t(\cdot)\|^2_{L^2(I)} + \|\cdot\|^2_{L^2(I)}\Big)^{\frac{1}{2}}, \tag{23}$$

and

$$\|\cdot\|_{{}^rH^\tau(I)} = \Big(\|{}_t\mathcal{D}^\tau_T(\cdot)\|^2_{L^2(I)} + \|\cdot\|^2_{L^2(I)}\Big)^{\frac{1}{2}}. \tag{24}$$

Let $2\tau \in (0, 1)$ and $\Omega = I \times \Lambda_d$. We define

$${}^l_0H^\tau\Big(I; L^2(\Lambda_d)\Big) := \Big\{u \mid \|u(t,\cdot)\|_{L^2(\Lambda_d)} \in H^\tau(I), u|_{t=0} = u|_{x=a_i} = u|_{x=b_i} = 0,\ i = 1, \cdots, d\Big\}, \tag{25}$$

which is equipped with the norm

$$\begin{aligned}
\|u\|_{{}^lH^\tau(I;L^2(\Lambda_d))} &= \Big\|\|u(t,\cdot)\|_{L^2(\Lambda_d)}\Big\|_{{}^lH^\tau(I)}\\
&= \Big(\|{}_0\mathcal{D}^\tau_t u\|^2_{L^2(\Omega)} + \|u\|^2_{L^2(\Omega)}\Big)^{\frac{1}{2}}.
\end{aligned} \tag{26}$$

Similarly,

$${}^r_0H^\tau\Big(I; L^2(\Lambda_d)\Big) := \Big\{v \mid \|v(t,\cdot)\|_{L^2(\Lambda_d)} \in H^\tau(I), v|_{t=T} = v|_{x=a_i} = v|_{x=b_i} = 0,\ i = 1, \cdots, d\Big\}, \tag{27}$$

which is equipped with the norm

$$\begin{aligned}
\|v\|_{{}^rH^\tau(I;L^2(\Lambda_d))} &= \Big\|\|v(t,\cdot)\|_{L^2(\Lambda_d)}\Big\|_{{}^rH^\tau(I)}\\
&= \Big(\|{}_t\mathcal{D}^\tau_T v\|^2_{L^2(\Omega)} + \|v\|^2_{L^2(\Omega)}\Big)^{\frac{1}{2}}.
\end{aligned} \tag{28}$$

We define the solution space

$$\mathcal{B}^{\tau,\nu_1,\cdots,\nu_d}(\Omega) := {}^l_0H^\tau\Big(I; L^2(\Lambda_d)\Big) \cap L^2(I; \mathcal{X}_d), \tag{29}$$

endowed with the norm

$$\|u\|_{\mathcal{B}^{\tau,\nu_1,\cdots,\nu_d}} = \left\{\|u\|^2_{{}^lH^\tau(I;L^2(\Lambda_d))} + \|u\|^2_{L^2(I;\mathcal{X}_d)}\right\}^{\frac{1}{2}}, \tag{30}$$

where due to (21),

$$\begin{aligned}
\|u\|_{L^2(I;\mathcal{X}_d)} &= \Big\|\|u(t,.)\|_{\mathcal{X}_d}\Big\|_{L^2(I)}\\
&= \left\{\|u\|^2_{L^2(\Omega)} + \sum_{i=1}^{d}\Big(\|{}_{x_i}\mathcal{D}^{\nu_i}_{b_i}(u)\|^2_{L^2(\Omega)} + \|{}_{a_i}\mathcal{D}^{\nu_i}_{x_i}(u)\|^2_{L^2(\Omega)}\Big)\right\}^{\frac{1}{2}}.
\end{aligned} \tag{31}$$

Therefore,

$$\|u\|_{\mathcal{B}^{\tau,\nu_1,\cdots,\nu_d}} = \left\{ \|u\|^2_{L^2(\Omega)} + \|\,{}_0\mathcal{D}^{\tau}_t\,(u)\|^2_{L^2(\Omega)} + \sum_{i=1}^{d} \left( \|\,{}_{x_i}\mathcal{D}^{\nu_i}_{b_i}\,(u)\|^2_{L^2(\Omega)} + \|\,{}_{a_i}\mathcal{D}^{\nu_i}_{x_i}\,(u)\|^2_{L^2(\Omega)} \right) \right\}^{\frac{1}{2}}. \tag{32}$$

Likewise, we define the test space

$$\mathfrak{B}^{\tau,\nu_1,\cdots,\nu_d}(\Omega) := {}^{r}_{0}H^{\tau}\Big(I; L^2(\Lambda_d)\Big) \cap L^2(I; \mathcal{X}_d), \tag{33}$$

endowed with the norm

$$\begin{aligned} \|v\|_{\mathfrak{B}^{\tau,\nu_1,\cdots,\nu_d}} &= \left\{ \|v\|^2_{{}^{r}H^{\tau}(I;L^2(\Lambda_d))} + \|v\|^2_{L^2(I;\mathcal{X}_d)} \right\}^{\frac{1}{2}} \\ &= \left\{ \|v\|^2_{L^2(\Omega)} + \|\,{}_t\mathcal{D}^{\tau}_T\,(v)\|^2_{L^2(\Omega)} + \sum_{i=1}^{d} \left( \|\,{}_{x_i}\mathcal{D}^{\nu_i}_{b_i}\,(v)\|^2_{L^2(\Omega)} + \|\,{}_{a_i}\mathcal{D}^{\nu_i}_{x_i}\,(v)\|^2_{L^2(\Omega)} \right) \right\}^{\frac{1}{2}}. \end{aligned} \tag{34}$$

In case $2\tau \in (1,2)$, we define the solution space as

$$\mathcal{B}^{\tau,\nu_1,\cdots,\nu_d}(\Omega) := {}^{l}_{0,0}H^{\tau}\Big(I; L^2(\Lambda_d)\Big) \cap L^2(I; \mathcal{X}_d), \tag{35}$$

where

$${}^{l}_{0,0}H^{\tau}\Big(I; L^2(\Lambda_d)\Big) := \left\{ u \mid \|u(t,\cdot)\|_{L^2(\Lambda_d)} \in H^{\tau}(I),\ \frac{\partial u}{\partial t}|_{t=0} = u|_{t=0} = u|_{x=a_i} = u|_{x=b_i} = 0,\ i = 1,\cdots,d \right\},$$

which is associated with $\|\cdot\|_{\mathcal{B}^{\tau,\nu_1,\cdots,\nu_d}(\Omega)}$. The corresponding test space is also defined as

$$\mathfrak{B}^{\tau,\nu_1,\cdots,\nu_d}(\Omega) := {}^{r}_{0,0}H^{\tau}\Big(I; L^2(\Lambda_d)\Big) \cap L^2(I; \mathcal{X}_d), \tag{36}$$

where

$${}^{r}_{0,0}H^{\tau}\Big(I; L^2(\Lambda_d)\Big) := \left\{ v \mid \|v(t,\cdot)\|_{L^2(\Lambda_d)} \in H^{\tau}(I),\ \frac{\partial v}{\partial t}|_{t=T} = v|_{t=T} = v|_{x=a_i} = v|_{x=b_i} = 0,\ i = 1,\cdots,d \right\},$$

which is endowed with $\|\cdot\|_{\mathfrak{B}^{\tau,\nu_1,\cdots,\nu_d}(\Omega)}$.

### 3.3. Petrov–Galerkin method

Next, we define the corresponding bilinear form as

$$\begin{aligned} a(u,v) = {} & ({}_0\mathcal{D}^{\tau}_t\,u,\,{}_t\mathcal{D}^{\tau}_T\,v)_{\Omega} + \sum_{i=1}^{d} \left[ c_{l_i} ({}_{a_i}\mathcal{D}^{\mu_i}_{x_i}\,u,\,{}_{x_i}\mathcal{D}^{\mu_i}_{b_i}\,v)_{\Omega} + c_{r_i} ({}_{x_i}\mathcal{D}^{\mu_i}_{a_i}\,u,\,{}_{a_i}\mathcal{D}^{\mu_i}_{x_i}\,v)_{\Omega} \right] \\ & - \sum_{j=1}^{d} \left[ \kappa_{l_j} ({}_{a_j}\mathcal{D}^{\nu_j}_{x_j}\,u,\,{}_{x_j}\mathcal{D}^{\nu_j}_{b_j}\,v)_{\Omega} + \kappa_{r_j} ({}_{x_j}\mathcal{D}^{\nu_j}_{b_j}\,u,\,{}_{a_j}\mathcal{D}^{\nu_j}_{x_j}\,v)_{\Omega} \right] + \gamma\,(u,v)_{\Omega}. \end{aligned} \tag{37}$$

Now, the problem reads as: find $u \in \mathcal{B}^{\tau,\nu_1,\cdots,\nu_d}(\Omega)$ such that

$$a(u,v) = (f,v)_{\Omega}, \quad \forall v \in \mathfrak{B}^{\tau,\nu_1,\cdots,\nu_d}(\Omega), \tag{38}$$

where $a(u,v)$ is a continuous bilinear form and $f \in (\mathcal{B}^{\tau,\nu_1,\cdots,\nu_d})^*(\Omega)$, which is the dual space of $\mathcal{B}^{\tau,\nu_1,\cdots,\nu_d}(\Omega)$. It should be noted that $({}_0\mathcal{D}^{2\tau}_t\,u,\,v)_{\Omega} = ({}_0\mathcal{D}^{\tau}_t\,u,\,{}_t\mathcal{D}^{\tau}_T\,v)_{\Omega}$ is proven in Proposition 1 in [59] and later in [60] requiring less regularity and constraint. Therefore, we construct a Petrov–Galerkin spectral method for $u \in \mathcal{B}^{\tau,\nu_1,\cdots,\nu_d}(\Omega)$, satisfying the weak form of (14) as

$$\begin{aligned} & ({}_0\mathcal{D}^{\tau}_t\,u,\,{}_t\mathcal{D}^{\tau}_T\,v)_{\Omega} + \sum_{i=1}^{d} \left[ c_{l_i} ({}_{a_i}\mathcal{D}^{\mu_i}_{x_i}\,u,\,{}_{x_i}\mathcal{D}^{\mu_i}_{b_i}\,v)_{\Omega} + c_{r_i} ({}_{a_i}\mathcal{D}^{\mu_i}_{x_i}\,v,\,{}_{x_i}\mathcal{D}^{\mu_i}_{b_i}\,u)_{\Omega} \right] \\ & \quad - \sum_{j=1}^{d} [k_{l_j} ({}_{a_j}\mathcal{D}^{\nu_j}_{x_j}\,u,\,{}_{x_j}\mathcal{D}^{\nu_j}_{b_j}\,v)_{\Omega} + k_{r_j} ({}_{a_j}\mathcal{D}^{\nu_j}_{x_j}\,v,\,{}_{x_j}\mathcal{D}^{\nu_j}_{b_j}\,u)_{\Omega}] \\ & \quad + \gamma\,(u,v)_{\Omega} = (f,v)_{\Omega}, \quad \forall v \in \mathfrak{B}^{\tau,\nu_1,\cdots,\nu_d}(\Omega), \end{aligned} \tag{39}$$

where $(\cdot,\cdot)_{\Omega}$ represents the usual $L^2$-product.

Next, we choose proper subspaces of $\mathcal{B}^{\tau,\nu_1,\cdots,\nu_d}(\Omega)$ and $\mathfrak{B}^{\tau,\nu_1,\cdots,\nu_d}(\Omega)$ as finite dimensional $U_N$ and $V_N$ with $\dim(U_N) = \dim(V_N) = N$. Now, the discrete problem reads: find $u_N \in U_N$ such that

$$a(u_N, v_N) = (f, v_N), \quad \forall v_N \in V_N. \tag{40}$$

By representing $u_N$ as a linear combination of points/elements in $U_N$, i.e., the corresponding $(1+d)$-dimensional space–time basis functions, the finite-dimensional problem (40) leads to a linear system known as *Lyapunov* system. For instance, when $d = 1$, we obtain the corresponding Lyapunov equation in the space–time domain $(0, T) \times (a_1, b_1)$ as

$$S_\tau \mathcal{U} M_1^T + c_{l_1} M_\tau \mathcal{U} S_{\mu_1,l}^T + c_{r_1} M_\tau \mathcal{U} S_{\mu_1,r}^T - \kappa_{l_1} M_\tau \mathcal{U} S_{\nu_1,l}^T - \kappa_{r_1} M_\tau \mathcal{U} S_{\nu_1,r}^T + \gamma M_\tau \mathcal{U} M_1^T = F, \tag{41}$$

where all are defined in 3.6. To find the general form of Lyapunov equation, we can define $S^{Tot}$ as

$$-\kappa_{l_1} S_{\nu_1,l} - \kappa_{r_1} S_{\nu_1,r} + c_{l_1} S_{\mu_1,l} + c_{r_1} S_{\mu_1,r} = S_1^{Tot}. \tag{42}$$

Considering equation (42), we obtain the (1+1)-D space–time Lyapunov system as

$$S_\tau \mathcal{U} M_1^T + M_\tau \mathcal{U} S_1^{Tot^T} + \gamma M_\tau \mathcal{U} M_1^T = F.$$

We present a new class of basis and test functions yielding *symmetric* stiffness matrices. Moreover, we compute exactly the corresponding mass matrices, which are either *symmetric* and *pentadiagonal*. In the following, we extensively study the properties of the aforementioned matrices, allowing us to formulate a general fast linear solver for (58).

### 3.4. Space of basis functions ($U_N$)

We construct the basis for the spatial discretization employing the Legendre polynomials defined as

$$\phi_m(\xi) = \sigma_m \left(P_{m+1}(\xi) - P_{m-1}(\xi)\right), \quad m = 1, 2, \cdots \quad \text{and } \xi \in [-1, 1], \tag{43}$$

where $\sigma_m = 2 + (-1)^m$. The definition reflects the fact that for $\mu_j \le 1/2$ and $1/2 \le \nu_j \le 1$, then both boundary conditions needs to be presented. Naturally, for the temporal basis functions only initial conditions are prescribed and the basis function for the temporal discretization is constructed based on the univariate poly-fractonomials [1] as

$$\psi_n^\tau(\eta) = \sigma_n (1+\eta)^\tau \; P_{n-1}^{-\tau,\tau}(\eta), \quad n = 1, 2, \cdots \quad \text{and } \eta \in [-1, 1], \tag{44}$$

for $n \ge 1$. With the notation established, we define the space–time trial space to be

$$U_N = span\left\{ \left(\psi_n^\tau \circ \eta\right)(t) \prod_{j=1}^{d} \left(\phi_{m_j} \circ \xi_j\right)(x_j) : n = 1, \ldots, \mathcal{N},\ m_j = 1, \ldots, \mathcal{M}_j \right\}, \tag{45}$$

where $\eta(t) = 2t/T - 1$ and $\xi_j(s) = 2\frac{s-a_j}{b_j-a_j} - 1$.

### 3.5. Space of test functions ($V_N$)

We construct the *spatial* test functions using Legendre polynomial as well as the basis function in the Petrov–Galerkin method as

$$\Phi_k(\xi) = \widetilde{\sigma}_k \left(P_{k+1}(\xi) - P_{k-1}(\xi)\right), \quad k = 1, 2, \cdots \quad \text{and } \xi \in [-1, 1], \tag{46}$$

where $\widetilde{\sigma}_k = 2(-1)^k + 1$. Next, we define the *temporal* test functions using the univariate poly-fractonomials

$$\Psi_r^\tau(\eta) = \widetilde{\sigma}_r (1-\eta)^\tau \; P_{r-1}^{\tau,-\tau}(\eta), \quad r = 1, 2, \cdots \quad \text{and } \eta \in [-1, 1], \tag{47}$$

and we construct the corresponding space–time test space as

$$V_N = span\left\{ \left(\Psi_r^\tau \circ \eta\right)(t) \prod_{j=1}^{d} \left(\Phi_{k_j} \circ \xi_j\right)(x_j) : r = 1, \ldots, \mathcal{N},\ k_j = 1, \ldots, \mathcal{M}_j \right\}. \tag{48}$$

**Remark 3.1.** The choices of $\sigma_m$ in (43) and (44), also $\widetilde{\sigma}_k$ in (46) and (47), result in the spatial/temporal mass and stiffness matrices being *symmetric*, which are discussed in Theorems 3.2, 3.3, and 3.4 in more details.

### 3.6. Implementation of PG spectral method

We now seek the solution to (14) in terms of a linear combination of elements in the space $U_N$ of the form

$$u_N(x,t)=\sum_{n=1}^{\mathcal{N}}\sum_{m_1=1}^{\mathcal{M}_1}\cdots\sum_{m_d=1}^{\mathcal{M}_d}\hat{u}_{n,m_1,\cdots,m_d}\Big[\psi_n^{\tau}(t)\prod_{j=1}^{d}\phi_{m_j}(x_j)\Big] \tag{49}$$

in $\Omega$. We enforce the corresponding residual

$$\begin{aligned}R_N(t,x_1,\cdots,x_d)={}&{}_0\mathcal{D}_t^{2\tau}u_N+\sum_{i=1}^{d}[c_{l_i\,a_i}\mathcal{D}_{x_i}^{2\mu_i}u_N+c_{r_i\,x_i}\mathcal{D}_{b_i}^{2\mu_i}u_N]-\sum_{j=1}^{d}[\kappa_{l_j\;\;a_j}\mathcal{D}_{x_j}^{2\nu_j}u_N+\kappa_{r_j\;\;x_j}\mathcal{D}_{b_j}^{2\nu_j}u_N]\\&+\gamma\,u_N-f\end{aligned} \tag{50}$$

to be $L^2$-orthogonal to $v_N\in V_N$, which leads to the finite-dimensional variational weak form in (40). Specifically, by choosing $v_N=\Psi_r^{\tau}(t)\prod_{j=1}^{d}\Phi_{k_j}(x_j)$, when $r=1,\ldots,\mathcal{N}$ and $k_j=1,\ldots,\mathcal{M}_j$, $j=1,2,\cdots,d$, we have

$$\begin{aligned}&\sum_{n=1}^{\mathcal{N}}\sum_{m_1=1}^{\mathcal{M}_1}\cdots\sum_{m_d=1}^{\mathcal{M}_d}\hat{u}_{n,m_1,\cdots,m_d}\Big(\{S_\tau\}_{r,n}\{M_1\}_{k_1,m_1}\cdots\{M_d\}_{k_d,m_d}+\sum_{i=1}^{d}[c_{l_i}\{M_\tau\}_{r,n}\{M_1\}_{k_1,m_1}\cdots\{S_{\nu_i,l}\}_{k_i,m_i}\cdots\{M_d\}_{k_d,m_d}\\&+c_{r_i}\{M_\tau\}_{r,n}\{M_1\}_{k_1,m_1}\cdots\{S_{\nu_i,r}\}_{k_i,m_i}\cdots\{M_d\}_{k_d,m_d}]-\sum_{j=1}^{d}\big[\kappa_{l_j}\{M_\tau\}_{r,n}\{M_1\}_{k_1,m_1}\cdots\{S_{\nu_j,l}\}_{k_j,m_j}\cdots\{M_d\}_{k_d,m_d}\\&+\kappa_{r_j}\{M_\tau\}_{r,n}\{M_1\}_{k_1,m_1}\cdots\{S_{\nu_j,r}\}_{k_j,m_j}\cdots\{M_d\}_{k_d,m_d}\big]+\gamma\{M_\tau\}_{r,n}\{M_1\}_{k_1,m_1}\cdots\{M_d\}_{k_d,m_d}\Big)\\&=F_{r,k_1,\cdots,k_d},\end{aligned} \tag{51}$$

where $S_\tau$ and $M_\tau$ denote, respectively, the temporal stiffness and mass matrices whose entries are defined as

$$\{S_\tau\}_{r,n}=\int_0^T{}_0\mathcal{D}_t^{\tau}\Big(\psi_n^{\tau}\circ\eta\Big)(t)\,{}_t\mathcal{D}_T^{\tau}\Big(\Psi_r^{\tau}\circ\eta\Big)(t)\,dt,$$

and

$$\{M_\tau\}_{r,n}=\int_0^T\Big(\Psi_r^{\tau}\circ\eta\Big)(t)\Big(\psi_n^{\tau}\circ\eta\Big)(t)\,dt.$$

Moreover, $S_{\mu_j}$ and $M_{\mu_j}$, $j=1,2,\cdots,d$, are the corresponding spatial stiffness and mass matrices where the left-sided and right-sided entries of the spatial stiffness matrices are obtained as

$$\{S_{\mu_j,l}\}_{k_j,m_j}=\int_{a_j}^{b_j}{}_{a_j}\mathcal{D}_{x_j}^{\mu_j}\Big(\phi_{m_j}\circ\xi_j\Big)(x_j)\;{}_{x_j}\mathcal{D}_{b_j}^{\mu_j}\Big(\Phi_{k_j}\circ\xi_j\Big)(x_j)\,dx_j=\{S_{\mu_j}\}_{k_j,m_j},$$

$$\{S_{\mu_j,r}\}_{k_j,m_j}=\int_{a_j}^{b_j}{}_{x_j}\mathcal{D}_{b_j}^{\mu_j}\Big(\phi_{m_j}\circ\xi_j\Big)(x_j)\;{}_{a_j}\mathcal{D}_{x_j}^{\mu_j}\Big(\Phi_{k_j}\circ\xi_j\Big)(x_j)\,dx_j=\{S_{\mu_j}\}_{k_j,m_j}^{T},$$

and the corresponding entries of the spatial mass matrix are given by

$$\{M_j\}_{k_j,m_j}=\int_{a_j}^{b_j}\Big(\Phi_{k_j}\circ\xi_j\Big)(x_j)\Big(\phi_{m_j}\circ\xi_j\Big)(x_j)\,dx_j.$$

Moreover, the components of the load vector are computed as

$$F_{r,k_1,\cdots,k_d}=\int_{\Omega}f(t,x_1,\cdots,x_d)\Big(\Psi_r^{\tau}\circ\eta\Big)(t)\prod_{j=1}^{d}\Big(\Phi_{k_j}\circ\xi_j\Big)(x_j)\,d\Omega. \tag{52}$$

The linear system (51) can be exhibited as the following general Lyapunov equation

$$\Big( S_\tau \otimes M_1 \otimes M_2 \cdots \otimes M_d + \sum_{i=1}^{d} c_{l_i} M_\tau \otimes M_1 \otimes \cdots \otimes S_{\mu_i,l} \otimes M_{i+1} \cdots \otimes M_d$$
$$+ \sum_{i=1}^{d} c_{r_i} M_\tau \otimes M_1 \otimes \cdots \otimes S_{\mu_i,r} \otimes M_{i+1} \cdots \otimes M_d - \sum_{i=1}^{d} \kappa_{l_i} M_\tau \otimes M_1 \otimes \cdots \otimes S_{\nu_i,l} \otimes M_{i+1} \cdots \otimes M_d$$
$$- \sum_{i=1}^{d} \kappa_{r_i} M_\tau \otimes M_1 \otimes \cdots \otimes S_{\nu_i,r} \otimes M_{i+1} \cdots \otimes M_d + \gamma\ M_\tau \otimes M_1 \otimes M_2 \cdots \otimes M_d \Big) \mathcal{U} = F. \tag{53}$$

Let

$$c_{l_i} \times S_{\mu_i,l} + c_{r_i} \times S_{\mu_i,r} - \kappa_{l_i} \times S_{\nu_i,l} - \kappa_{r_i} \times S_{\nu_i,r} = S_i^{Tot}. \tag{54}$$

Considering the fact that all the aforementioned stiffness and mass matrices are *symmetric*, $S_{\mu_i,l}$, $S_{\mu_i,r}$, $S_{\nu_i,l}$, and $S_{\nu_i,r}$ can be replaced by $S_i^{Tot}$ which remains symmetric. Therefore,

$$\Big( S_\tau \otimes M_1 \otimes M_2 \cdots \otimes M_d + \sum_{i=1}^{d} [\ M_\tau \otimes M_1 \otimes \cdots \otimes M_{i-1} \otimes S_i^{Tot} \otimes M_{i+1} \cdots \otimes M_d\ ]$$
$$+ \gamma\ M_\tau \otimes M_1 \otimes M_2 \cdots \otimes M_d \Big) \mathcal{U} = F, \tag{55}$$

in which $\otimes$ represents the Kronecker product, $F$ denotes the multi-dimensional load matrix whose entries are given in (52), and $\mathcal{U}$ denotes the corresponding multi-dimensional matrix of unknown coefficients with entries $\hat{u}_{n,m_1,\cdots,m_d}$.

In the Theorems 3.2, 3.3, and 3.4, we study the properties of the aforementioned matrices. Besides, we present efficient ways of deriving the spatial mass and the temporal stiffness matrices analytically and exact computation of the temporal mass and the spatial stiffness matrices through proper quadrature rules.

**Theorem 3.2.** The temporal stiffness matrix $S_\tau$ corresponding to the time-fractional order $\tau \in (0, 1)$ is a diagonal $\mathcal{N} \times \mathcal{N}$ matrix, whose entries are obtained as

$$\{S_\tau\}_{r,n} = \widetilde{\sigma}_r\, \sigma_n \frac{\Gamma(n+\tau)}{\Gamma(n)} \frac{\Gamma(r+\tau)}{\Gamma(r)} \Big(\frac{2}{T}\Big)^{2\tau-1} \frac{2}{2n-1} \delta_{r,n}, \quad r, n = 1, 2, \cdots, \mathcal{N}.$$

Moreover, the entries of temporal mass matrices $M_\tau$ can be computed exactly by employing a Gauss–Lobatto–Jacobi (GLJ) rule with respect to the weight function $(1-\eta)^\tau (1+\eta)^\tau$, $\eta \in [-1, 1]$, where $\alpha = \tau/2$. Moreover, $M_\tau$ is symmetric.

**Proof.** See [49]. □

**Theorem 3.3.** The spatial mass matrix $M$ is a pentadiagonal $\mathcal{M} \times \mathcal{M}$ matrix, whose entries are explicitly given as

$$M_{k,r} = \widetilde{\sigma}_k\, \sigma_r \Big[ \frac{2}{2k+3} \delta_{k,r} - \frac{2}{2k+3} \delta_{k+1,r-1} - \frac{2}{2k-3} \delta_{k-1,r+1} + \frac{2}{2k-3} \delta_{k-1,r-1} \Big]. \tag{56}$$

**Proof.** The (k, r)*th*-entry of the spatial mass matrix is given by

$$M_{k,r} = \int_a^b \phi_r \circ \xi(x)\, \Phi_k \circ \xi(x)\, dx = \Big(\frac{b-a}{2}\Big) \int_{-1}^{1} \phi_r(\xi) \Phi_k(\xi)\, d\xi, \tag{57}$$

where $\xi = 2\frac{x-a}{b-a} - 1$ and $\xi \in (-1, 1)$. Substituting the spatial basis/test functions, we have

$$M_{k,r} = \Big(\frac{b-a}{2}\Big) \widetilde{\sigma}_k\, \sigma_r \big[ \widetilde{M}_{k,r} - \widetilde{M}_{k+1,r-1} - \widetilde{M}_{k-1,r+1} + \widetilde{M}_{k,r} \big], \tag{58}$$

in which

$$\widetilde{M}_{i,j} = \int_{-1}^{1} P_i(\xi)\, P_j(\xi)\, d\xi = \frac{2}{2i+1} \delta_{ij}. \tag{59}$$

Therefore, we have

$$M_{k,r} = \big(\frac{b-a}{2}\big)\,\widetilde{\sigma}_k\,\sigma_r\Big[\frac{2}{2k+3}\delta_{k,r} - \frac{2}{2k+3}\delta_{k+1,r-1} - \frac{2}{2k-3}\delta_{k-1,r+1} + \frac{2}{2k-3}\delta_{k,r}\Big]$$

as a pentadiagonal matrix. Moreover,

$$\begin{aligned} M_{r,k} &= \big(\frac{b-a}{2}\big)\,\widetilde{\sigma}_r\,\sigma_k\Big[\frac{2}{2r+3}\delta_{r,k} - \frac{2}{2r+3}\delta_{r+1,k-1} - \frac{2}{2r-3}\delta_{r-1,k+1} + \frac{2}{2r-3}\delta_{r,k}\Big] \\ &= M_{k,r}. \quad \square \end{aligned}$$

**Theorem 3.4.** The total spatial stiffness matrix $S_i^{Tot}$ is symmetric and its entries can be exactly computed as:

$$c_{l_i} \times S_{\mu_i,l} + c_{r_i} \times S_{\mu_i,r} - \kappa_{l_i} \times S_{\nu_i,l} - \kappa_{r_i} \times S_{\nu_i,r} = S_i^{Tot}, \tag{60}$$

where $i = 1, 2, \cdots, d$.

**Proof.** Regarding the definition of stiffness matrix, we have

$$\begin{aligned} \{S_{\mu_i,l}\}_{r,n} &= \int_{a_i}^{b_i} {}_{a_i}\mathcal{D}_{x_i}^{\mu_i}\Big(\phi_n \circ \xi_i(x_i)\Big)\,{}_{x_i}\mathcal{D}_{b_i}^{\mu_i}\Big(\Phi_r \circ \xi_i(x_i)\Big)\,dx_i, \\ &= \big(\frac{b_i-a_i}{2}\big)^{-2\mu_i+1}\widetilde{\sigma}_r\,\sigma_n \int_{-1}^{1} {}_{-1}\mathcal{D}_{\xi_i}^{\mu_i}\Big(P_{n+1}(\xi_i) - P_{n-1}(\xi_i)\Big)\,{}_{\xi_i}\mathcal{D}_{1}^{\mu_i}\Big(P_{k+1}(\xi_i) - P_{k-1}(\xi_i)\Big)\,d\xi_i \\ &= \big(\frac{b_i-a_i}{2}\big)^{-2\mu_i+1}\widetilde{\sigma}_r\,\sigma_n\Big[\widetilde{S}^{\mu_i}_{r+1,n+1} - \widetilde{S}^{\mu_i}_{r+1,n-1} - \widetilde{S}^{\mu_i}_{r-1,n+1} + \widetilde{S}^{\mu_i}_{r-1,n-1}\Big], \end{aligned}$$

where

$$\begin{aligned} \widetilde{S}^{\mu_i}_{r,n} &= \int_{-1}^{1} {}_{-1}\mathcal{D}_{\xi_i}^{\mu_i}\Big(P_n(\xi_i)\Big)\,{}_{\xi_i}\mathcal{D}_{1}^{\mu_i}\Big(P_r(\xi_i)\Big)\,d\xi_i \\ &= \int_{-1}^{1} \frac{\Gamma(r+1)}{\Gamma(r-\mu_i+1)}\,\frac{\Gamma(n+1)}{\Gamma(n-\mu_i+1)}\,(1+\xi_i)^{-\mu_i}(1-\xi_i)^{-\mu_i}\,P_r^{-\mu_i,\mu_i}(\xi_i)\,P_n^{\mu_i,-\mu_i}(\xi_i)d\xi_i. \end{aligned}$$

$\widetilde{S}^{\mu_i}_{r,n}$ can be computed accurately using Gauss–Jacobi quadrature rule as

$$\widetilde{S}^{\mu_i}_{r,n} = \frac{\Gamma(r+1)}{\Gamma(r-\mu_i+1)}\,\frac{\Gamma(n+1)}{\Gamma(n-\mu_i+1)}\sum_{q=1}^{\mathcal{Q}} w_q\;P_r^{-\mu_i,\,\mu_i}(\xi_q)P_n^{\mu_i,\,-\mu_i}(\xi_q), \tag{61}$$

in which $\mathcal{Q} \geq \mathcal{N}+2$ represents the minimum number of GJ quadrature points $\{\xi_q\}_{q=1}^{\mathcal{Q}}$, associated with the weigh function $(1-\xi_q)^{-\mu_i}(1+\xi_q)^{-\mu_i}$, for *exact* quadrature, and $\{w_q\}_{q=1}^{\mathcal{Q}}$ are the corresponding quadrature weights. Employing the property of the Jacobi polynomials where $P_n^{\alpha,\beta}(-x_i) = (-1)^n P_n^{\beta,\alpha}(x_i)$, we can re-express $\widetilde{S}^{\mu_i}_{r,n}$ as $(-1)^{(r+n)}\,\widetilde{S}^{\mu_i}_{n,r}$. Accordingly,

$$\begin{aligned} \{S_{\mu_i}\}_{r,n} &= \big(\frac{b_i-a_i}{2}\big)^{-2\mu_i+1}\widetilde{\sigma}_r\,\sigma_n\Big[(-1)^{(n+r+2)}\,\widetilde{S}^{\mu_i}_{n+1,r+1} - (-1)^{(n+r)}\,\widetilde{S}^{\mu_i}_{n+1,r-1} \\ &\qquad -(-1)^{(n+r)}\,\widetilde{S}^{\mu_i}_{n-1,r+1} + (-1)^{(n+r-2)}\,\widetilde{S}^{\mu_i}_{n-1,r-1}\Big] \\ &= \widetilde{\sigma}_r\,\sigma_n\,(-1)^{(n+r)}\Big[\widetilde{S}^{\mu_i}_{n+1,r+1} - \widetilde{S}^{\mu_i}_{n+1,r-1} - \widetilde{S}^{\mu_i}_{n-1,r+1} + \widetilde{S}^{\mu_i}_{n-1,r-1}\Big]. \end{aligned} \tag{62}$$

According to (62),

$$\{S_{\mu_i}\}_{r,n} = \{S_{\mu_i}\}_{n,r} \times \frac{\widetilde{\sigma}_r\,\sigma_n}{\widetilde{\sigma}_n\,\sigma_r}(-1)^{(n+r)}. \tag{63}$$

In fact, $\widetilde{\sigma}_r$ and $\sigma_n$ are chosen such that $(-1)^{(n+r)}$ is canceled. Furthermore,

$$\{S_{\mu_i,r}\}_{r,n} = \int_{a_i}^{b_i} {}_{a_i}\mathcal{D}_{x_i}^{\mu_i}\Big(\Phi_r(x_i)\Big)\, {}_{x_i}\mathcal{D}_{b_i}^{\mu_i}\Big(\phi_n(x_i)\Big)\, dx_i,$$
$$= \int_{a_i}^{b_i} {}_{a_i}\mathcal{D}_{x_i}^{\mu_i}\Big(\phi_n(x_i)\Big)\, {}_{x_i}\mathcal{D}_{b_i}^{\mu_i}\Big(\Phi_r(x_i)\Big)\, dx_i,$$
$$= \{S_{\mu_i,l}\}_{n,r}, \tag{64}$$

where $\{S_{\mu_i,l}\}_{n,r} = \{S_{\mu_i,l}\}_{r,n} = \{S_{\mu_i,r}\}_{r,n} = \{S_{\mu_i}\}_{r,n}$ due to symmetry of $S_{\mu_i,l}$ and $S_{\mu_i,r}$. Similar to (64), we get $\{S_{\nu_i,l}\}_{r,n} = \{S_{\nu_i,r}\}_{r,n} = \{S_{\nu_i}\}_{r,n}$; therefore,

$$-(\kappa_{l_i} + \kappa_{r_i})\, S_{\nu_i} + (c_{l_i} + c_{r_i})\, S_{\mu_i} = S_i^{Tot}. \tag{65}$$

Hence it can be easily concluded that the stiffness matrix $S_{n,r}^{\mu_i}$, $S_{n,r}^{\nu_i}$ and thereby $\{S_i^{Tot}\}_{n,r}$ as the sum of two symmetric matrices are symmetric. □

## 4. Unified fast FPDE solver

We formulate a closed-form solution for the Lyapunov system (55) in terms of the generalized eigensolutions that can be computed very efficiently, leading to the following unified fast solver for the development of Petrov–Galerkin spectral method.

**Theorem 4.1.** Let $\{\vec{e}^{\,j}, \lambda^{j}\}_{m_j=1}^{\mathcal{M}_j}$ be the set of general eigen-solutions of the spatial stiffness matrix $S_j^{Tot}$ with respect to the mass matrix $M_j$. Moreover, let $\{\vec{e}^{\,\tau}, \lambda^{\tau}\}_{n=1}^{\mathcal{N}}$ be the set of general eigen-solutions of the temporal mass matrix $M_\tau$ with respect to the stiffness matrix $S_\tau$. (I) if $d > 1$, then the multi-dimensional matrix of unknown coefficients $\mathcal{U}$ is explicitly obtained as

$$\mathcal{U} = \sum_{n=1}^{\mathcal{N}} \sum_{m_1=1}^{\mathcal{M}_1} \cdots \sum_{m_d=1}^{\mathcal{M}_d} \kappa_{n,m_1,\cdots,m_d}\, \vec{e}_n^{\,\tau} \otimes \vec{e}_{m_1}^{\,1} \otimes \cdots \otimes \vec{e}_{m_d}^{\,d}, \tag{66}$$

where $\kappa_{n,m_1,\cdots,m_d}$ are given by

$$\kappa_{n,m_1,\cdots,m_d} = \frac{(\vec{e}_n^{\,\tau}\, \vec{e}_{m_1}^{\,1} \cdots \vec{e}_{m_d}^{\,d})F}{\Big[(\vec{e}_n^{\,\tau^T} S_\tau \vec{e}_n^{\,\tau}) \prod_{j=1}^{d} ((\vec{e}_{m_j}^{\,j})^T M_j \vec{e}_{m_j}^{\,j})\Big] \Lambda_{n,m_1,\cdots,m_d}}, \tag{67}$$

in which the numerator represents the standard multi-dimensional inner product, and $\Lambda_{n,m_1,\cdots,m_d}$ are obtained in terms of the eigenvalues of all mass matrices as

$$\Lambda_{n,m_1,\cdots,m_d} = \Big[(1 + \gamma\ \lambda_n^{\tau}) + \lambda_n^{\tau} \sum_{j=1}^{d} (\lambda_{m_j}^{j})\Big].$$

(II) If $d = 1$, then the two-dimensional matrix of the unknown solution $\mathcal{U}$ is obtained as

$$\mathcal{U} = \sum_{n=1}^{\mathcal{N}} \sum_{m_1=1}^{\mathcal{M}_1} \kappa_{n,m_1}\, \vec{e}_n^{\,\tau}\ (\vec{e}_{m_1}^{\,1})^T,$$

where $\kappa_{n,m_1}$ is explicitly obtained as

$$\kappa_{n,m_1} = \frac{\vec{e}_n^{\,\tau^T} F\, \vec{e}_{m_1}^{\,1}}{(\vec{e}_n^{\,\tau^T} S_\tau \vec{e}_n^{\,\tau})((\vec{e}_{m_1}^{\,1})^T M_1 \vec{e}_{m_1}^{\,1}) \Big[(1 + \gamma\ \lambda_n^{\tau}) + \lambda_n^{\tau}\, \lambda_{m_1}^{1}\Big]}.$$

**Proof.** Let us consider the following generalized eigenvalue problems as

$$S_j^{Tot}\, \vec{e}_{m_j}^{\,j} = \lambda_{m_j}^{j}\, M_j\, \vec{e}_{m_j}^{\,j}, \quad m_j = 1, \cdots, \mathcal{M}_j, \quad j = 1, 2, \cdots, d, \tag{68}$$

and

$$M_\tau\, \vec{e}_n^{\,\tau} = \lambda_n^{\tau}\, S_\tau\, \vec{e}_n^{\,\tau}, \quad n = 1, 2, \cdots, \mathcal{N}. \tag{69}$$

Having the spatial and temporal eigenvectors determined in equations (69) and (68), we can represent the unknown coefficient matrix $\mathcal{U}$ in (49) in terms of the aforementioned eigenvectors as

$$\mathcal{U}=\sum_{n=1}^{\mathcal{N}}\sum_{m_1=1}^{\mathcal{M}_1}\cdots\sum_{m_d=1}^{\mathcal{M}_d}\kappa_{n,m_1,\cdots,m_d}\,\vec{e}_n^{\,\tau}\otimes\vec{e}_{m_1}^{\,1}\otimes\cdots\otimes\vec{e}_{m_d}^{\,d},\tag{70}$$

where $\kappa_{n,m_1,\cdots,m_d}$ are obtained as follows. First, we take the multi-dimensional inner product of $\vec{e}_q^{\,\tau}\,\vec{e}_{p_1}^{\,1}\cdots\vec{e}_{p_d}^{\,d}$ on both sides of the Lyapunov equation (55) as

$$\begin{aligned}&(\vec{e}_q^{\,\tau}\,\vec{e}_{p_1}^{\,1}\,\vec{e}_{p_2}^{\,2}\cdots\vec{e}_{p_d}^{\,d})\Big[\,S_\tau\otimes M_1\otimes\cdots\otimes M_d+\sum_{j=1}^{d}[M_\tau\otimes M_1\otimes\cdots\otimes M_{j-1}\otimes S_j^{Tot}\otimes M_{j+1}\cdots\otimes M_d]\\&+\gamma\;M_\tau\otimes M_1\otimes\cdots\otimes M_d\Big]\mathcal{U}=(\vec{e}_q^{\,\tau}\,\vec{e}_{p_1}^{\,1}\cdots\vec{e}_{p_d}^{\,d})F.\end{aligned}$$

Then, by replacing (68) and (69) into (67) and re-arranging the terms, we get

$$\begin{aligned}&\sum_{n=1}^{\mathcal{N}}\sum_{m_1=1}^{\mathcal{M}_1}\cdots\sum_{m_d=d}^{\mathcal{M}_d}\kappa_{n,m_1,\cdots,m_d}\times\Big(\,\vec{e}_q^{\,\tau^T}S_\tau\vec{e}_n^{\,\tau}\;\;(\vec{e}_{p_1}^{\,1})^TM_1\vec{e}_{m_1}^{\,1}\;\;\cdots\;\;(\vec{e}_{p_d}^{\,d})^TM_d\,\vec{e}_{m_d}^{\,d}\\&\quad+\sum_{j=1}^{d}\vec{e}_q^{\,\tau^T}M_\tau\vec{e}_n^{\,\tau}\,(\vec{e}_{p_1}^{\,1})^TM_1\vec{e}_{m_1}^{\,1}\cdots(\vec{e}_{p_j}^{\,j})^TS_j^{Tot}\vec{e}_{m_j}^{\,j}\,(\vec{e}_{p_{j+1}}^{\,j+1})^TM_{j+1}\vec{e}_{m_{j+1}}^{\,j+1}\cdots(\vec{e}_{p_d}^{\,d})^TM_d\vec{e}_{m_d}^{\,d}\\&\quad+\gamma\;\vec{e}_q^{\,\tau^T}M_\tau\vec{e}_n^{\,\tau}\,(\vec{e}_{p_1}^{\,1})^TM_1\vec{e}_{m_1}^{\,1}\,(\vec{e}_{p_1}^{\,2})^TM_2\vec{e}_{m_2}^{\,2}\cdots(\vec{e}_{p_d}^{\,d})^TM_d\vec{e}_{m_d}^{\,d}\Big)\\&\quad=(\vec{e}_q^{\,\tau}\,\vec{e}_{p_1}^{\,1}\,\vec{e}_{p_2}^{\,2}\cdots\vec{e}_{p_d}^{\,d})F.\end{aligned}$$

Recalling that $S_j^{Tot}\vec{e}_{m_j}^{\,j}=(\lambda_{m_j}^{j}M_j\,\vec{e}_{m_j}^{\,j})$ and $M_\tau\,\vec{e}_n^{\,\tau}=(\lambda_n^\tau\,S_\tau\,\vec{e}_n^{\,\tau})$, we have

$$\begin{aligned}&\sum_{n=1}^{\mathcal{N}}\sum_{m_1=1}^{\mathcal{M}_1}\cdots\sum_{m_d=1}^{\mathcal{M}_d}\kappa_{n,m_1,\cdots,m_d}\Big(\vec{e}_q^{\,\tau^T}S_\tau\vec{e}_n^{\,\tau}\,(\vec{e}_{p_1}^{\,1})^TM_1\vec{e}_{m_1}^{\,1}\,(\vec{e}_{p_2}^{\,2})^TM_2\vec{e}_{m_2}^{\,2}\cdots(\vec{e}_{p_d}^{\,d})^TM_d\,\vec{e}_{m_d}^{\,d}\\&\quad+\sum_{j=1}^{d}\vec{e}_q^{\,\tau^T}(\lambda_n^\tau\,S_\tau\,\vec{e}_n^{\,\tau})\,(\vec{e}_{p_1}^{\,1})^TM_1\vec{e}_{m_1}^{\,1}\cdots(\vec{e}_{p_j}^{\,j})^T(\lambda_{m_j}^{j}M_j\vec{e}_{m_j}^{\,j})\cdots(\vec{e}_{p_d}^{\,d})^TM_d\,\vec{e}_{m_d}^{\,d}\\&\quad+\gamma\;\vec{e}_q^{\,\tau^T}(\lambda_n^\tau\,S_\tau\,\vec{e}_n^{\,\tau})\,(\vec{e}_{p_1}^{\,1})^TM_1\vec{e}_{m_1}^{\,1}\,(\vec{e}_{p_2}^{\,2})^TM_2\vec{e}_{m_2}^{\,2}\cdots(\vec{e}_{p_d}^{\,d})^TM_d\vec{e}_{m_d}^{\,d}\Big)\\&\quad=(\vec{e}_q^{\,\tau}\,\vec{e}_{p_1}^{\,1}\,\vec{e}_{p_2}^{\,2}\cdots\vec{e}_{p_d}^{\,d})F.\end{aligned}$$

Therefore,

$$\kappa_{n,m_1,\cdots,m_d}=\frac{(\vec{e}_n^{\,\tau}\,\vec{e}_{m_1}^{\,1}\cdots\vec{e}_{m_d}^{\,d})F}{\Big[(\vec{e}_n^{\,\tau^T}S_\tau\vec{e}_n^{\,\tau})\prod_{j=1}^{d}((\vec{e}_{m_j}^{\,j})^TM_j\vec{e}_{m_j}^{\,j})\Big]\times\Big[(1+\gamma\;\lambda_n^\tau)+\lambda_n^\tau\sum_{j=1}^{d}(\lambda_{m_j}^{j})\Big]}.$$

Then, we have

$$\begin{aligned}&\sum_{n=1}^{\mathcal{N}}\sum_{m_1=1}^{\mathcal{M}_1}\cdots\sum_{m_d=1}^{\mathcal{M}_d}\kappa_{n,m_1,\cdots,m_d}\,(\vec{e}_q^{\,\tau^T}S_\tau\vec{e}_n^{\,\tau})((\vec{e}_{p_1}^{\,1})^TM_1\vec{e}_{m_1}^{\,1})\cdots((\vec{e}_{p_d}^{\,d})^TM_d\vec{e}_{m_d}^{\,d})\\&\quad\times\Big[(1+\gamma\;\lambda_n^\tau)+\lambda_n^\tau\sum_{j=1}^{d}(\lambda_{m_j}^{j})\Big]=(\vec{e}_q^{\,\tau}\,\vec{e}_{p_1}^{\,1}\,\vec{e}_{p_2}^{\,2}\cdots\vec{e}_{p_d}^{\,d})F.\end{aligned}$$

Due to the fact that the spatial Mass $M_j$ and temporal stiffness matrices $S_\tau$ are diagonal (see Theorems 3.3 and 3.2), we have $(\vec{e}_q^{\,\tau^T}S_\tau\vec{e}_n^{\,\tau})=0$ if $q\neq n$, and also $((\vec{e}_{p_j}^{\,j})^TM_j\vec{e}_{m_j}^{\,j})=0$ if $p_j\neq m_j$, which completes the proof for the case $d>1$.

Following similar steps for the two-dimensional problem, it is easy to see that if $d=1$, the relationship for $\kappa$ can be derived as

$$\kappa_{q,p_1}=\frac{\vec{e}_q^{\,\tau^T}F\,\vec{e}_{p_1}^{\,1}}{(\vec{e}_q^{\,\tau^T}S_\tau\vec{e}_q^{\,\tau})((\vec{e}_{p_1}^{\,1})^TM_1\vec{e}_{p_1}^{\,1})\Big[(1+\gamma\;\lambda_n^\tau)+\lambda_n^\tau\,\lambda_{m_1}^{1}\Big]}.\tag{71}$$

In section 4.1, we present a computational method for the fast solver which reduces the computational cost significantly. □

### 4.1. Computational considerations

Employing the fast solver in $(1+d)$ dimensional problem $d \geq 1$ reduces the dominant computational cost of the eigensolver from $\mathcal{O}(N^{2(1+d)})$ to $\mathcal{O}(N^{2+d})$, which becomes even more efficient in higher dimensional problems. This approach is extensively discussed in [49].

## 5. Numerical tests

We now examine the unified PG spectral method and the corresponding unified fast solver (70) and (71) for (14) in the context of several numerical test cases in order to investigate the spectral/exponential rate of convergence in addition to the computational efficiency of the scheme. The corresponding force term $f$ in (14) is obtained in Appendix for the following test cases, listed as:

**Test case (I):** (smooth solutions with finite regularity) we consider the following exact solution to perform the temporal *p-refinement* as

$$u^{exact} = t^{p_1} \times \Big( (1+x_1)^{p_2} - \epsilon (1+x_1)^{p_3} \Big), \tag{72}$$

where $p_1 = 7\frac{2}{3}$, $p_2 = 6\frac{1}{3}$, $p_3 = 6\frac{2}{7}$ and $t \in [0,\ 2]$ and $x_1 \in [-1,\ 1]$.

**Test case (II):** (spatially smooth function) we consider

$$u^{exact} = t^{p_1} \times sin[n\pi\ (1+x_1)], \tag{73}$$

where $n = 1$ and $p_1 = 6\frac{1}{3}$, for the exponential *p-refinement*.

**Test case (III):** (high-dimensional problems) to perform the *p-refinement* in higher dimensions ($d = 2,\ 3$), we choose the exact solution

$$u^{exact} = t^{p_1} \times \prod_{i=1}^{d} \Big( (1+x_i)^{p_{2i}} - \epsilon_i (1+x_i)^{p_{2i+1}} \Big), \tag{74}$$

where $p_1 = 7\frac{2}{3}$, $p_2 = 6\frac{1}{3}$, $p_3 = 6\frac{2}{7}$, $p_4 = 7\frac{4}{5}$, $p_5 = 7\frac{1}{7}$, $p_6 = 7\frac{3}{5}$, $p_7 = 7\frac{1}{7}$ and $\epsilon_1 = 2^{p_2 - p_3}$, $\epsilon_2 = 2^{p_4 - p_5}$, $\epsilon_3 = 2^{p_6 - p_7}$ in the hypercube domain as $[0,\ 1] \times \underbrace{[-1,\ 1] \times \cdots \times [-1,\ 1]}_{d\ times}$.

**Test case (IV):** (CPU time) to examine the efficiency of the method for the high-dimensional domain, we employ (74), where $p_1 = 4$, $p_{2i} = 3\frac{1}{3}$, $p_{2i+1} = 3\frac{2}{7}$, $\epsilon_i = 2^{p_{2i} - p_{2i+1}}$, $t \in [0, 2]$, and $x_i \in [-1, 1]$. In the following numerical examples, we illustrate the convergence rate and efficiency of the method, employing the test cases.

### 5.1. Numerical test (I)

We plot the log–log scale $L^2$-error versus temporal orders $\mathcal{N}$ in Fig. 1 in a log–log scale plot for the test case (I) while $2\tau = \frac{1}{10},\ \frac{9}{10},\ 2\mu_1 = \frac{5}{10},\ 2\nu_1 = \frac{15}{10},\ T = 2$ and spatial expansion order is fixed ($\mathcal{M}_1 = 23$). Having the same set-up, we also consider $2\tau = \frac{11}{10},\ \frac{19}{10}$ in the temporal direction to examine the spectral convergence of fractional wave equation. The $L^2$-error decays linearly in the log–log scale plot as temporal expansion order $\mathcal{N}$ increases in both cases, indicating the spectral convergence of PG method. In [2], we obtain the theoretical convergence rate of $\|e\|_{L^2}$ and compare with the corresponding practical ones.

### 5.2. Numerical test (II)

Here, we perform the spatial *p-refinement* while the temporal expansion order is fixed for the test case (I). In Fig. 2, spectral convergence of log–log scale $L^2$-error versus spatial expansion orders $\mathcal{M}_1$ is shown where $2\nu_1 = \frac{11}{10},\ \frac{19}{10}$ in setup (a). We set $2\tau = \frac{6}{10},\ 2\mu_1 = \frac{5}{10},\ T = 2$ and temporal expansion order is fixed ($\mathcal{N} = 23$). In this case, the limit fractional orders of $\nu_1$ are examined, where both have the spectral convergence but with different rates. We also carry out the spatial *p-refinement* for the limit fractional orders of $\mu_1$. The spectral convergence of the PG method is observed, where $2\mu_1 = \frac{1}{10},\ \frac{9}{10}$ and $2\nu_1 = \frac{15}{10}$. To this end, we can conclude that the PG method in (1+1) dimensional space–time domain is spectrally accurate up to the order of $10^{-15}$.

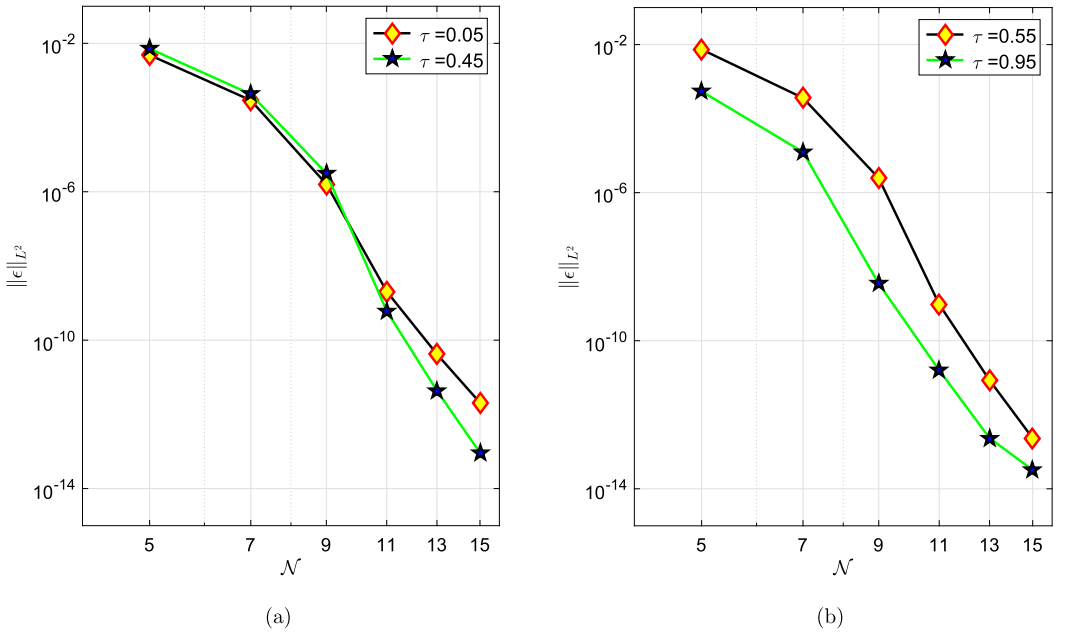


**Fig. 1.** Temporal *p-refinement*: log–log scale $L^2$-error versus temporal expansion orders $\mathcal{N}$ for test case (I).

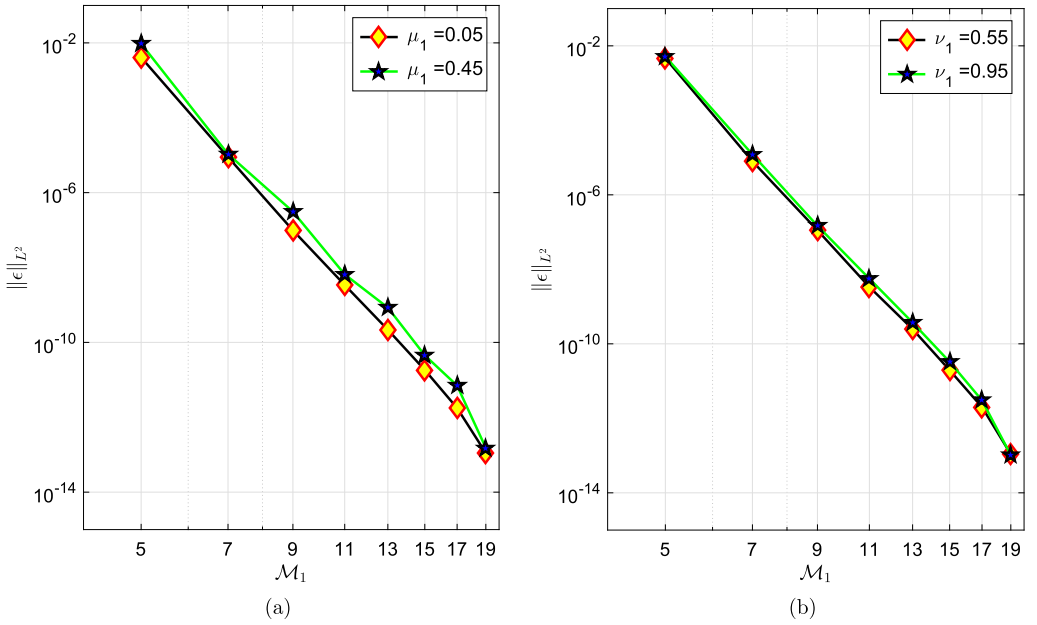


**Fig. 2.** Spatial *p-refinement*: log–log scale $L^2$-error versus spatial expansion orders $\mathcal{M}$ for the test case (I).

### 5.3. Numerical test (III)

In Fig. 3, we plot $\|e\|_{L^2} = \|u - u^{ext}\|_{L^2}$ versus spatial expansion orders $\mathcal{M}_1$ for the test case (II), showing the spatial *p-refinement*. In setup (a) $2\nu_1 = \frac{11}{10}$, $\frac{19}{10}$ and $2\mu_1 = \frac{5}{10}$ and in setup (b) $2\mu_1 = \frac{1}{10}$, $\frac{9}{10}$ and $2\nu_1 = \frac{15}{10}$ where $2\tau = \frac{6}{10}$. The temporal expansion order ($\mathcal{N} = 23$) is fixed. The exponential convergence in the log-linear scale plot is illustrated clearly for the limit fractional orders of $\mu_1$ and $\nu_1$ in case spatial component of the exact solution is a sinusoidal smooth function.

### 5.4. Numerical test (IV)

In addition to spatial/temporal *p-refinement*, we perform *p-refinement* for (1+2) and (1+3) as the higher dimensional domain in the test case (III). In Fig. 4, the spectral convergence of log–log $L^\infty$-error versus spatial expansion orders $\mathcal{M}_2$,

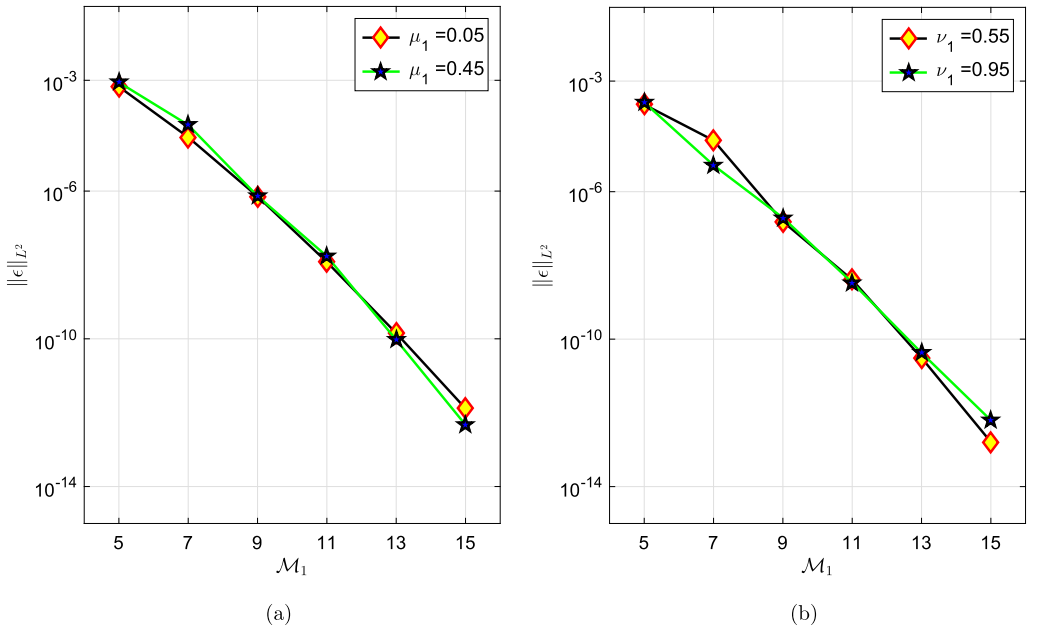


**Fig. 3.** Exponential convergence in the spatial *p-refinement*: log–log scale $L^2$-error versus spatial expansion orders $\mathcal{M}$ for the test case (II).

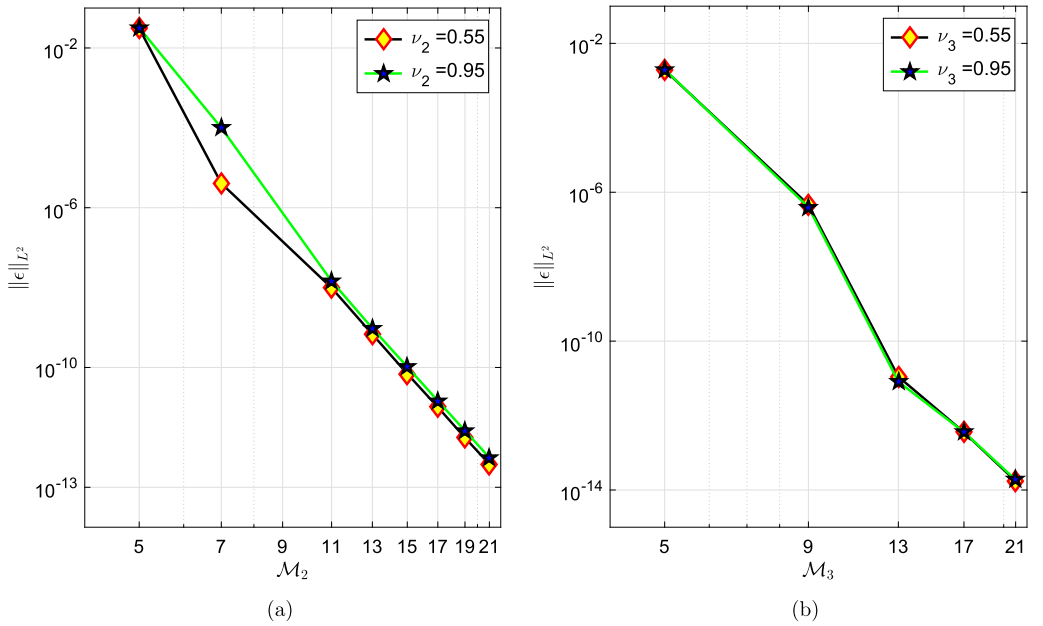


**Fig. 4.** Spatial *p-refinement*: log–log scale $L^\infty$-error versus spatial expansion orders $\mathcal{M}_2$, $\mathcal{M}_3$ in the test case (III) for the limit fractional orders of $\nu$.

$\mathcal{M}_3$ is shown. In setup (a), $2\nu_2 = \frac{11}{10}$, $\frac{19}{10}$ while $2\nu_1 = \frac{15}{10}$, $2\mu_1 = \frac{4}{10}$ and $2\mu_2 = \frac{6}{10}$ and setup (b) $2\nu_3 = \frac{11}{10}$, $\frac{19}{10}$ while $2\nu_1 = \frac{14}{10}$, $2\nu_2 = \frac{16}{10}$, $2\mu_1 = \frac{3}{10}$, $2\mu_2 = \frac{5}{10}$ and $2\mu_3 = \frac{7}{10}$, where $2\tau = \frac{6}{10}$, $T = 2$. Furthermore, we increase the maximum bases order uniformly in all dimensions.

Similarly, we perform the spatial *p-refinement* for the limit fractional orders of $\mu_2$ and $\mu_3$ in FADE. We study setup (a) $2\mu_2 = \frac{1}{10}$, $\frac{9}{10}$ while $2\mu_1 = \frac{5}{10}$, and setup (b) $2\mu_3 = \frac{1}{10}$, $\frac{9}{10}$ while $2\mu_1 = \frac{4}{10}$, $2\mu_2 = \frac{6}{10}$. In both setups, $2\tau = \frac{6}{10}$, $2\nu_1 = \frac{5}{10}$, $2\nu_2 = \frac{5}{10}$, $T = 2$. Furthermore, $\mathcal{N} = \mathcal{M}_1 = \mathcal{M}_2 = \mathcal{M}_3$ changes concurrently. In Fig. 5, the PG method shows spectral convergence for the limit fractional orders of $\mu_2$ and $\mu_3$.

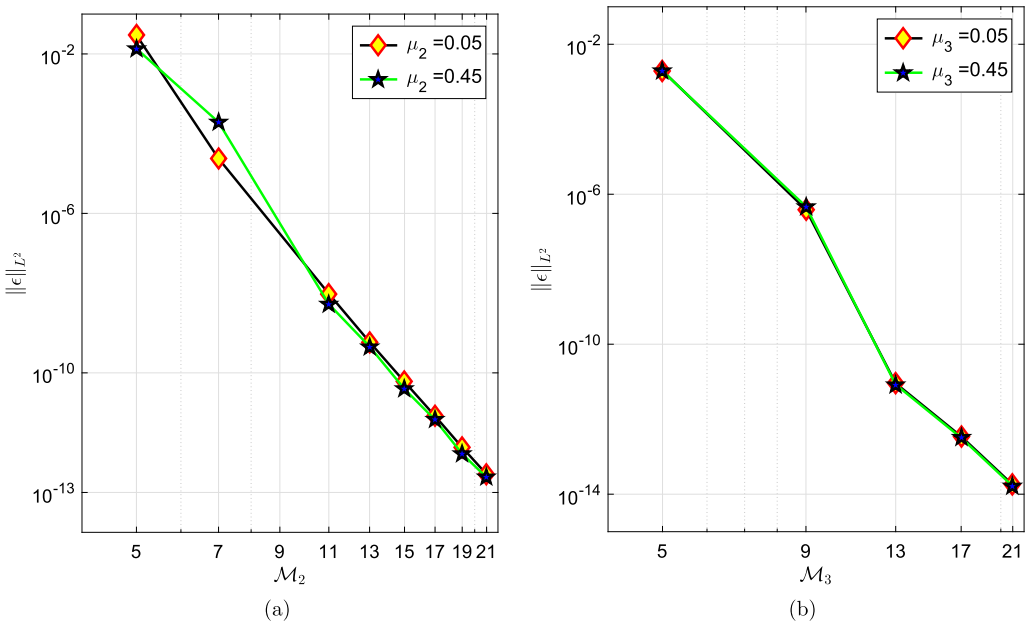


**Fig. 5.** Spatial *p-refinement*: log–log scale $L^\infty$-error versus spatial expansion orders $\mathcal{M}_2$, $\mathcal{M}_3$ for the test case (III) for the limit fractional orders of $\mu$.

**Table 1**
Performance study and CPU time (in sec.) of the unified PG spectral method for the test case (IV). In each step, we uniformly increase the bases order by one in all dimensions ($\mathcal{N} = \mathcal{M}_1 = \mathcal{M}_2 = \mathcal{M}_3$).

| 2-D FADRE | | |
|---|---|---|
| $\mathcal{N}$ | $\|\epsilon\|_{L^\infty}$ | CPU time [sec] |
| 5 | 0.008 | 1.48 |
| 7 | 0.0003 | 3.01 |
| 9 | $1.69 \times 10^{-6}$ | 3.48 |
| 15 | $2.96 \times 10^{-11}$ | 4.95 |

| 3-D FADRE | | |
|---|---|---|
| $\mathcal{N}$ | $\|\epsilon\|_{L^\infty}$ | CPU time [sec] |
| 5 | 0.01 | 1.43 |
| 7 | 0.0003 | 5.39 |
| 9 | $2.6 \times 10^{-7}$ | 6.14 |
| 15 | $2.41 \times 10^{-10}$ | 7.54 |

| 4-D FADRE | | |
|---|---|---|
| $\mathcal{N}$ | $\|\epsilon\|_{L^\infty}$ | CPU time [sec] |
| 5 | 0.00005 | 3.56 |
| 7 | $3.31 \times 10^{-7}$ | 8.87 |
| 9 | $8.17 \times 10^{-9}$ | 5.37 |
| 15 | $9.70 \times 10^{-12}$ | 55.78 |

### *5.5. Numerical test (V)*

To examine the efficiency of the PG method and the fast solver in high-dimensional problem, the convergence results and CPU time for test case (IV) are presented in Table 1 for (1+1), (1+3) and (1+5) dimensional space–time hypercube domains where the error is measured by the essential norm $\|e\|_\infty$ in the test case (IV). The CPU time is obtained on Intel (Xeon E52670) 2.5 GHz processor. The presented PG method remains spectrally accurate in (1+5) dimensional time–space domain.

## 6. Summary and discussion

### *6.1. Summary*

We developed a new unified Petrov–Galerkin spectral method for a class of fractional partial differential equations with constant coefficients (14) in a $(1+d)$-dimensional *space–time* hypercube, $d = 1, 2, 3$, etc, subject to homogeneous Dirichlet initial/boundary conditions. We employed *Jacobi poly-fractonomials*, as temporal basis/test functions, and the Legendre polynomials as spatial basis/test functions, yielding spatial mass matrices being independent of the spatial fractional orders. Additionally, we formulated the novel unified fast linear solver for the resulting high-dimensional linear system, which reduces the computational cost significantly. In fact, the main idea of the paper was to formulate a closed-form solution for the high-dimensional Lyapunov equation in terms of the eigensolutions up to the precision accuracy of computationally obtained eigensolutions. The PG method has been illustrated to be spectrally accurate for power-law test cases in each dimension. Furthermore, exponential convergence is observed for a sinusoidal smooth function in a spatial *p*-refinement. To check the stability and spectral convergence of the PG method, we carried out the corresponding well-posedness, discrete stability and error analysis of the method for (38) in [2].

Despite the high accuracy and the efficiency of the method especially in higher-dimensional problems, treatment of FPDEs in complex geometries and FPDEs with variable coefficients will be studies in our future works.

**Acknowledgements**

This work was supported by the AFOSR Young Investigator Program (YIP) award on: "Data-Infused Fractional PDE Modelling and Simulation of Anomalous Transport" (FA9550-17-1-0150) and by the MURI/ARO on Fractional PDEs for Conservation Laws and Beyond: Theory, Numerics and Applications (W911NF-15-1-0562).

**Appendix**

Here, we provide the force function based on the exact solutions.

*.2. Force term of test case (I)*

To obtain $f$ in (14) based on (72), first we need to calculate all fractional derivatives of $u^{ext}$. To satisfy the corresponding boundary conditions, $\epsilon_i = 2^{p_{2i}-p_{2i+1}}$. Take $X^T = t^{p_1}$ and $X_i^S = (1+\zeta_i)^{p_{2i}} - \epsilon_i (1+\zeta_i)^{p_{2i+1}}$, where $\zeta_i = 2\frac{x_i - a_i}{b_i - a_i} - 1$ and $\zeta_i \in [-1, 1]$. Considering (2),

$$ {}_0\mathcal{D}_t^{2\tau} X^T = \frac{\Gamma[p_1+1]}{\Gamma[p_1+1-2\tau]} t^{p_1-2\tau} = (\frac{T}{2})^{p_1-2\tau} \frac{\Gamma[p_1+1]}{\Gamma[p_1+1-2\tau]} (1+\eta(t))^{p_1-2\tau}, \tag{75} $$

where $\eta(t) = 2(\frac{t}{T}) - 1$. Similarly,

$$ \begin{aligned} {}_{a_i}\mathcal{D}_{x_i}^{2\mu_i} X_i^S = \Big(\frac{b_i-a_i}{2}\Big)^{-2\mu_i} \Big[ & \frac{\Gamma[p_{2i}+1]}{\Gamma[p_{2i}+1-2\mu_i]} (1+\zeta_{2i}(x_i))^{p_{2i}-2\mu_i} \\ & - \epsilon_i \frac{\Gamma[p_{2i+1}+1]}{\Gamma[p_{2i+1}+1-2\mu_i]} (1+\zeta_{2i}(x_i))^{p_{2i+1}-2\mu_i} \Big], \end{aligned} \tag{76} $$

and

$$ \begin{aligned} {}_{a_i}\mathcal{D}_{x_i}^{2\nu_i} X_i^S = \Big(\frac{b_i-a_i}{2}\Big)^{-2\nu_i-2} \Big[ & \frac{\Gamma[p_{2i}+1]}{\Gamma[p_{2i}+1-2\nu_i]} (1+\zeta_{2i}(x_i))^{p_{2i}-2\nu_i} \\ & - \epsilon_i \frac{\Gamma[p_{2i+1}+1]}{\Gamma[p_{2i+1}+1-2\nu_i]} (1+\zeta_{2i}(x_i))^{p_{2i+1}-2\nu_i} \Big]. \end{aligned} \tag{77} $$

Therefore,

$$ \begin{aligned} f = {} & (\frac{T}{2})^{p_1-2\tau} \frac{\Gamma[p_1+1]}{\Gamma[p_1+1-2\tau]} (1+\eta)^{p_1-2\tau} \prod_{i=1}^{d} (1+\zeta_i)^{p_{2i}} - \epsilon_i (1+\zeta_i)^{p_{2i+1}} \\ & + \sum_{i=1} (\frac{T}{2})^{p_1} (1+\eta)^{p_1} \Big( c_{l_i} \Big(\frac{b_i-a_i}{2}\Big)^{-2\mu_i} \Big[ \frac{\Gamma[p_{2i}+1]}{\Gamma[p_{2i}+1-2\mu_i]} (1+\zeta_{2i})^{p_{2i}-2\mu_i} \\ & - \epsilon_i \frac{\Gamma[p_{2i+1}+1]}{\Gamma[p_{2i+1}+1-2\mu_i]} (1+\zeta_{2i})^{p_{2i+1}-2\mu_i} \Big] \prod_{j=1,\, j\neq i}^{d} [(1+\zeta_j)^{p_{2j}} - \epsilon_j (1+\zeta_j)^{p_{2j+1}}] \Big) \\ & - \sum_{i=1} (\frac{T}{2})^{p_1} (1+\eta)^{p_1} \Big( \kappa_{l_i} \Big(\frac{b_i-a_i}{2}\Big)^{-2\nu_i-2} \Big[ \frac{\Gamma[p_{2i}+1]}{\Gamma[p_{2i}+1-2\mu_i]} (1+\zeta_{2i})^{p_{2i}-2\nu_i} \\ & - \epsilon_i \frac{\Gamma[p_{2i+1}+1]}{\Gamma[p_{2i+1}+1-2\nu_i]} (1+\zeta_{2i})^{p_{2i+1}-2\nu_i} \Big] \prod_{j=1,\, j\neq i}^{d} [(1+\zeta_j)^{p_{2j}} - \epsilon_j (1+\zeta_j)^{p_{2j+1}}] \Big). \end{aligned} \tag{78} $$

*.3. Force term of test case (II)*

Take $X^T = t^{p_1}$ and $X^S = sin(n\pi\zeta_1)$. Here, we approximate $X^S$ as

$$ X^S = \Sigma_{j=1}^{N_s} (-1)^{2j-1} \frac{(n\pi\zeta_1)^{2j-1}}{(2j-1)!}, \tag{79} $$

where $N_s$ controls the level of approximation error. Taking the same steps of (78), we obtain

$$f = (\frac{T}{2})^{p_1-2\tau} \frac{\Gamma[p_1+1]}{\Gamma[p_1+1-2\tau]} (1+\eta)^{p_1-2\tau} \Sigma_{j=1}^{N_s} (-1)^{2j-1} \frac{(n\pi\zeta_1)^{2j-1}}{(2j-1)!}$$
$$+ (\frac{T}{2})^{p_1} (1+\eta)^{p_1} \Big[ (c_{l_1}) \Big( \frac{b_1-a_1}{2} \Big)^{-2\mu_1} \Sigma_{j=1}^{N_s} (-1)^{2j-1} \frac{(n\pi\zeta_1)^{2j-1}}{(2j-1)!} \frac{\Gamma[2j]}{\Gamma[2j-2\mu_1]} \zeta^{2j-2\mu_1}$$
$$- (\kappa_{l_1}) \Big( \frac{b_1-a_1}{2} \Big)^{-2\nu_1-2} \Sigma_{j=1}^{N_s} (-1)^{2j-1} \frac{(n\pi\zeta_1)^{2j-1}}{(2j-1)!} \frac{\Gamma[2j]}{\Gamma[2j-2\nu_1]} \zeta^{2j-2\nu_1} \Big]. \quad (80)$$

## References


[1] M. Zayernouri, G.E. Karniadakis, Fractional Sturm–Liouville eigen-problems: theory and numerical approximation, J. Comput. Phys. 252 (2013) 495–517.
[2] M. Samiee, M. Zayernouri, M.M. Meerschaert, A unified spectral method for FPDEs with two-sided derivatives; part II: stability and error analysis, submitted for publication, arXiv preprint, arXiv:1710.08337, 2017.
[3] I. Podlubny, Fractional Differential Equations: an Introduction to Fractional Derivatives, Fractional Differential Equations, to Methods of Their Solution and Some of Their Applications, Fractional Differential Equations, vol. 198, Academic Press, 1998.
[4] M.M. Meerschaert, A. Sikorskii, Stochastic Models for Fractional Calculus, De Gruyter Studies in Mathematics, vol. 43, Walter de Gruyter, 2012.
[5] B. Guo, X. Pu, F. Huang, Fractional Partial Differential Equations and Their Numerical Solutions, World Scientific, 2015.
[6] S.G. Samko, A.A. Kilbas, O.I. Marichev, Fractional Integrals and Derivatives: Theory and Applications, Gordon and Breach, Yverdon, 1993.
[7] A. Carpinteri, F. Mainardi, Fractals and Fractional Calculus in Continuum Mechanics, Springer, 2014.
[8] R. Klages, G. Radons, I.M. Sokolov, Anomalous Transport: Foundations and Applications, Wiley–VCH, 2008.
[9] R. Metzler, J. Klafter, The random walk's guide to anomalous diffusion: a fractional dynamics approach, Phys. Rep. 339 (1) (2000) 1–77.
[10] G.M. Zaslavsky, J. Meiss, Physics of chaos in Hamiltonian systems, Nature 398 (6725) (1999) 303.
[11] P. Perdikaris, G.E. Karniadakis, Fractional-order viscoelasticity in one-dimensional blood flow models, Ann. Biomed. Eng. 42 (5) (2014) 1012–1023.
[12] R.L. Magin, Fractional Calculus in Bioengineering, Begell House, Redding, 2006.
[13] B.M. Regner, Randomness in Biological Transport, Ph.D. thesis, University of California, San Diego, 2014.
[14] M. Naghibolhosseini, Estimation of Outer–Middle Ear Transmission Using DPOAEs and Fractional-Order Modeling of Human Middle Ear, Ph.D. thesis, City University of New York, New York, NY, 2015.
[15] M. Naghibolhosseini, G.R. Long, Fractional-order modelling and simulation of human ear, Int. J. Comput. Math. (2017) 1–17.
[16] T. Solomon, E.R. Weeks, H.L. Swinney, Observation of anomalous diffusion and Lévy flights in a two-dimensional rotating flow, Phys. Rev. Lett. 71 (24) (1993) 3975.
[17] T. Solomon, E.R. Weeks, H.L. Swinney, Chaotic advection in a two-dimensional flow: Lévy flights and anomalous diffusion, Phys. D, Nonlinear Phenom. 76 (1) (1994) 70–84.
[18] M.M. Meerschaert, F. Sabzikar, M.S. Phanikumar, A. Zeleke, Tempered fractional time series model for turbulence in geophysical flows, J. Stat. Mech. Theory Exp. 2014 (9) (2014) P09023.
[19] D. del Castillo-Negrete, B. Carreras, V. Lynch, Fractional diffusion in plasma turbulence, Phys. Plasmas 11 (8) (2004) 3854–3864.
[20] D. del Castillo-Negrete, P. Morrison, Chaotic transport by Rossby waves in shear flow, Phys. Fluids A, Fluid Dyn. 5 (4) (1993) 948–965.
[21] D.A. Benson, R. Schumer, M.M. Meerschaert, S.W. Wheatcraft, Fractional dispersion, Lévy motion, and the MADE tracer tests, in: Dispersion in Heterogeneous Geological Formations, Springer, 2001, pp. 211–240.
[22] D.A. Benson, S.W. Wheatcraft, M.M. Meerschaert, Application of a fractional advection–dispersion equation, Water Resour. Res. 36 (6) (2000) 1403–1412.
[23] K. Vafai, Handbook of Porous Media, CRC Press, 2015.
[24] F. Mainardi, Fractional Calculus and Waves in Linear Viscoelasticity: an Introduction to Mathematical Models, World Scientific, 2010.
[25] C. Lubich, Discretized fractional calculus, SIAM J. Math. Anal. 17 (3) (1986) 704–719.
[26] N. Sugimoto, Burgers equation with a fractional derivative; hereditary effects on nonlinear acoustic waves, J. Fluid Mech. 225 (1991) 631–653.
[27] N. Sugimoto, Generalized Burgers equations and fractional calculus, Nonlinear Wave Motion 408 (1989) 162–179.
[28] M.M. Meerschaert, C. Tadjeran, Finite difference approximations for fractional advection–dispersion flow equations, J. Comput. Appl. Math. 172 (1) (2004) 65–77.
[29] C. Tadjeran, M.M. Meerschaert, A second-order accurate numerical method for the two-dimensional fractional diffusion equation, J. Comput. Phys. 220 (2) (2007) 813–823.
[30] H. Hejazi, T. Moroney, F. Liu, A finite volume method for solving the two-sided time–space fractional advection–dispersion equation, Open Phys. 11 (10) (2013) 1275–1283.
[31] M. Chen, W. Deng, A second-order numerical method for two-dimensional two-sided space fractional convection diffusion equation, Appl. Math. Model. 38 (13) (2014) 3244–3259.
[32] F. Zeng, C. Li, F. Liu, I. Turner, Numerical algorithms for time-fractional subdiffusion equation with second-order accuracy, SIAM J. Sci. Comput. 37 (1) (2015) A55–A78.
[33] X. Zhao, Z.-z. Sun, G.E. Karniadakis, Second-order approximations for variable order fractional derivatives: algorithms and applications, J. Comput. Phys. 293 (2015) 184–200.
[34] D. Li, C. Zhang, M. Ran, A linear finite difference scheme for generalized time fractional Burgers equation, Appl. Math. Model. 40 (11) (2016) 6069–6081.
[35] L. Feng, P. Zhuang, F. Liu, I. Turner, J. Li, High-order numerical methods for the Riesz space fractional advection–dispersion equations, Comput. Math. Appl. (2016).
[36] F. Zeng, Z. Zhang, G.E. Karniadakis, Fast difference schemes for solving high-dimensional time-fractional subdiffusion equations, J. Comput. Phys. 307 (2016) 15–33.
[37] M. Zayernouri, A. Matzavinos, Fractional Adams–Bashforth/Moulton methods: an application to the fractional Keller–Segel chemotaxis system, J. Comput. Phys. 317 (2016) 1–14.
[38] J. Shen, L.-L. Wang, Fourierization of the Legendre–Galerkin method and a new space–time spectral method, Appl. Numer. Math. 57 (5) (2007) 710–720.
[39] N. Sweilam, M. Khader, M. Adel, Chebyshev pseudo-spectral method for solving fractional advection–dispersion equation, Appl. Math. 5 (19) (2014) 3240.
[40] F. Chen, Q. Xu, J.S. Hesthaven, A multi-domain spectral method for time-fractional differential equations, J. Comput. Phys. 293 (2015) 157–172.
[41] P. Mokhtary, Discrete Galerkin method for fractional integro-differential equations, Acta Math. Sci. 36 (2) (2016) 560–578.
[42] E. Kharazmi, M. Zayernouri, Fractional pseudo-spectral methods for distributed-order fractional PDEs, Int. J. Comput. Math. (2017) 1–22, https://doi.org/10.1080/00207160.2017.1421949.
[43] E. Kharazmi, M. Zayernouri, G.E. Karniadakis, A Petrov–Galerkin spectral element method for fractional elliptic problems, Comput. Methods Appl. Mech. Eng. 324 (2017) 512–536.

[44] A. Lischke, M. Zayernouri, G.E. Karniadakis, A Petrov–Galerkin spectral method of linear complexity for fractional multiterm ODEs on the half line, SIAM J. Sci. Comput. 39 (3) (2017) A922–A946.
[45] M. Zayernouri, M. Ainsworth, G.E. Karniadakis, Tempered fractional Sturm–Liouville eigenproblems, SIAM J. Sci. Comput. 37 (4) (2015) A1777–A1800.
[46] M. Zayernouri, W. Cao, Z. Zhang, G.E. Karniadakis, Spectral and discontinuous spectral element methods for fractional delay equations, SIAM J. Sci. Comput. 36 (6) (2014) B904–B929.
[47] M. Zayernouri, G.E. Karniadakis, Exponentially accurate spectral and spectral element methods for fractional ODEs, J. Comput. Phys. 257 (2014) 460–480.
[48] M. Zayernouri, G.E. Karniadakis, Fractional spectral collocation method, SIAM J. Sci. Comput. 36 (1) (2014) A40–A62.
[49] M. Zayernouri, M. Ainsworth, G.E. Karniadakis, A unified Petrov–Galerkin spectral method for fractional PDEs, Comput. Methods Appl. Mech. Eng. 283 (2015) 1545–1569.
[50] M. Zayernouri, G.E. Karniadakis, Fractional spectral collocation methods for linear and nonlinear variable order FPDEs, J. Comput. Phys. 293 (2015) 312–338.
[51] M. Dehghan, M. Abbaszadeh, A. Mohebbi, Analysis of two methods based on Galerkin weak form for fractional diffusion-wave: meshless interpolating element free Galerkin (IEFG) and finite element methods, Eng. Anal. Bound. Elem. 64 (2016) 205–221.
[52] M. Dehghan, M. Abbaszadeh, A. Mohebbi, The use of element free Galerkin method based on moving Kriging and radial point interpolation techniques for solving some types of Turing models, Eng. Anal. Bound. Elem. 62 (2016) 93–111.
[53] L. Zhao, W. Deng, J.S. Hesthaven, Spectral methods for tempered fractional differential equations, Math. Comput. (2016).
[54] S. Chen, J. Shen, L.-L. Wang, Generalized Jacobi functions and their applications to fractional differential equations, Math. Comput. 85 (300) (2016) 1603–1638.
[55] Z. Mao, J. Shen, Efficient spectral-Galerkin methods for fractional partial differential equations with variable coefficients, J. Comput. Phys. 307 (2016) 243–261.
[56] J.F.R. Askey, Integral representations for Jacobi polynomials and some applications, J. Math. Anal. Appl. 26 (1969).
[57] B. Baeumer, T. Luks, M.M. Meerschaert, Space–time fractional Dirichlet problems, arXiv preprint, arXiv:1604.06421.
[58] X. Li, C. Xu, Existence and uniqueness of the weak solution of the space–time fractional diffusion equation and a spectral method approximation, Commun. Comput. Phys. 8 (5) (2010) 1016–1051.
[59] H. Zhang, F. Liu, V. Anh, Galerkin finite element approximation of symmetric space-fractional partial differential equations, Appl. Math. Comput. 217 (6) (2010) 2534–2545.
[60] E. Kharazmi, M. Zayernouri, G.E. Karniadakis, Petrov–Galerkin and spectral collocation methods for distributed order differential equations, SIAM J. Sci. Comput. 39 (3) (2017) A1003–A1037.